AN ANALOG COMPUTER FOR THE CALCULATION OF PARTICLE TRAJECTORIES AND BEAM EMITTANCE ENVELOPES

by

NADHIM M. M. AL-QAZZAZ

B.Sc., University of Wales, 1958

A THESIS SUBMITTED IN PARTIAL FULFILLMENT
OF THE REQUIREMENTS FOR THE DEGREE OF
MASTER OF SCIENCE
in the Department
of
Physics

We accept this thesis as conforming
to the required standard

[redacted]

Accepted by the Faculty of Graduate Studies

on Sept 25/1969 by [redacted] Dean of Faculty

August, 1969

ABSTRACT

Supervisor: Dr. L.P. Robertson

An analog computer system that calculates the trajectories of charged particles emitted from a source and moving under the influence of magnetic fields in a beam transport system, was extended so that it is capable of calculating the extent of a beam consisting of a group of charged particle trajectories, that is, the beam envelope. For this purpose, a function generator unit was developed and some modifications were made in the computer.

This computer can be used to calculate beam envelopes, as well as particle trajectories, for a beam transport system containing nine distinct active elements in both the horizontal and vertical planes. It can operate repetitively in two speeds and the output can be displayed on an oscilloscope, recorded graphically on an xy - plotter, or read on a digital voltmeter.

Sample problems and an example on the use of the computer for designing beam transport systems are included. The error was found by comparison to results obtained on a digital computer to be within (2.0% ± 0.2 volts) for trajectory calculations and (2.4% ± 0.2 volts) for envelope calculations. The constant represents the noise in the system.

TABLE OF CONTENTS

ACKNOWLEDGEMENTS

The author wishes to thank Dr. L.P. Robertson for his guidance during the progress of the work, and to thank Dr. R.M. Pearce, Dr. J.L. Climenhaga, and Dr. S. Ryce for reading the draft.

Financial support from the TRIUMF project and from the University of Victoria, in the form of a University of Victoria Graduate Fellowship, is gratefully acknowledged.

The analog computer described in this thesis was provided by CRNL, Chalk River.

LIST OF TABLES

LIST OF FIGURES

1. INTRODUCTION

A beam transport system is a collection of magnetic devices arranged in such a manner that they are capable of containing and directing a diverging beam of charged particles emitted from a source such as an accelerator or target and travelling to an experiment.

If the direction of motion is taken along the z-axis, the equation of motion to be solved can be written as (Steffen, 1964)

$$\frac{d^2u}{dz^2} + k(z)u - d = 0 \qquad (2.3.1)$$

where u = x or y and represents the displacements along the two directions transverse to the direction of motion; k(z) will depend on the type of device used; d represents momentum dispersion when a bending magnet or a similar dispersive device is present.

However, it is often more useful to study the behavior of a beam of particles rather than the trajectory of a single particle. This is particularly true for beam matching and optimizing purposes. In this case, the equation to be solved is (Steffen, 1964)

$$\frac{d^2E}{dz^2} + k(z)E - \frac{\varepsilon^2}{E^3} = 0 \qquad (2.4.2)$$

where E is called the envelope function and represents the extent of the beam in either of the two planes transverse to the direction of motion.

The development of equations (2.3.1) and (2.4.2), and the meaning and significance of the various terms and symbols appearing in them, are discussed in Chapter 2.

The design and study of beam transport systems involve solving the above two equations and this task can be simplified and carried out rapidly by using analog computers. They offer two main advantages over digital computational techniques: firstly, speed, and secondly, the ease of adjusting the various parameters and immediately observing, on an oscilloscope, the effects of these adjustments on the particle or beam behaviour. The use of the analog computation applied to the solution of the beam transport equations is discussed in Chapter 3.

The computer described here is a commercial, general purpose analog computer with a digital timing system*. It was assembled by Louis (1967) for solving equation (2.3.1) for single particle trajectories.

To solve equation (2.4.2), one has to generate a non-linear function to represent the last term of this equation. The generation of this function and the consequent modifications and extension of the computer to make it capable of solving equation (2.4.2), as well as (2.3.1), forms the subject matter of this work. This problem is discussed in Chapter 3.

---

* Systron Donner Model 10/20, Systron Donner Co., Concord, California 94520.

The capability of the modified computer and the accuracy obtained are discussed in Chapter 4. In Chapter 5, sample problems and a design problem are included to illustrate the uses of the computer.

This work is an extension of that of Louis (1967) and, since the basic features of the computer described by him remain unaltered, reference will be made to his thesis for details on some topics.

2. BASIC CONCEPTS OF BEAM TRANSPORT SYSTEMS

2.1 Definitions and Notation

In a beam transport system, a beam of particles is focussed and its direction controlled by a series of magnetic devices which are separated by field-free spaces called drift spaces. These devices and drift spaces are referred to as beam transport elements.

A charged particle in a magnetic field is subject to the Lorentz force

$$\overline{F} = e\overline{v} \times \overline{B} \qquad (2.1.1)$$

where e is the charge on the particle, v its velocity, and B the magnetic field. The Lorentz force acts in a plane orthogonal to the direction of motion and therefore causes the particle to be displaced from its initial path.

The path followed by the particle under the influence of the applied fields is called the particle "trajectory". The "optical axis" or central trajectory is defined for a given initial position and direction. Trajectory coordinates for particles with other initial conditions are referred to this central trajectory.

If, as is the case for many beams, the angular deviations from the optical axis, θ, are small, then the approximation $\sin\theta = \theta$ is valid. This is referred to as the paraxial approximation.

In developing the equations of motion, sufficient accuracy is often obtained if only the linear terms in the displacement and angle are retained (Steffen, 1964). This will be referred to as the linear approximation and the resulting equations as the linearised equations of motion. The symmetry properties of the quadrupoles and magnets chosen as beam transport elements, and discussed in Section 2.2, permit the assumption of independent equations for the x- and y-motions.

2.2 Beam Handling Devices

The most commonly used beam handling elements are the quadrupoles and bending magnets (Banford, 1966).

2.2.1 Quadrupoles

Quadrupoles are used as "lenses" for containing the beam of particles transported between the source and the experimental area. A quadrupole magnet consists of four symmetrically placed iron pole pieces mounted on a common yoke and excited by current carrying coils. An ideal quadrupole would have a symmetric field as shown in Fig. 1.

The components of the quadrupole field are (Banford, 1966)

$$B_x = gy \ , \qquad B_y = gx \ , \qquad (2.2.1)$$

and $$B_z = 0,$$

where $$g = \frac{\partial B_x}{\partial y} = \frac{\partial B_y}{\partial x} = \text{constant}.$$

g is known as the magnetic field gradient of the quadrupole. Then the components of the Lorentz force (2.1.1) are

$$F_x \simeq +evB_y = +evgx \ , \qquad F_y \simeq -evB_x = -evgy \qquad (2.2.2)$$

by using (2.2.1).

Therefore $$F_x = -F_y$$

i.e. if the force has a focussing effect in the xz-plane, it will have a defocussing effect in the yz-plane. This action can be reversed by rotating the quadrupole through 90^o so that the north and south poles are interchanged. A net focussing effect in both planes can be obtained by using two quadrupoles, one of each type.

The first order equations of motion of a charged particle travelling through a quadrupole, assuming paraxial conditions, are obtained (Banford, 1966) from equations (2.1.1), (2.2.1), and (2.2.2),

thus from (2.1.1)

$$F_x = e(v_y B_z - v_z B_y) = -ev_z B_y$$

so $$m \frac{d^2x}{dt^2} = -ev_z gx$$

from equation (2.2.2).

With the approximation

$$v = \frac{ds}{dt} \simeq \frac{dz}{dt} ,$$

$$mv^2 \frac{d^2x}{dz^2} = -evgx .$$

Therefore $$\frac{d^2x}{dz^2} = - \frac{e}{p} gx .$$

Similarly for the y-plane. The equations of motion are

$$\frac{d^2x}{dz^2} + \frac{g(z)}{(B\rho)} x = 0$$

in the focussing plane, and (2.2.3)

$$\frac{d^2y}{dz^2} - \frac{g(z)}{(B\rho)} y = 0$$

in the defocussing plane, where $(B\rho)$ is known as the "magnetic rigidity" and is related to the particle momentum by

$$(B\rho) = \frac{mv}{e} = \frac{p}{e} ,$$

m being the relativistic mass of the particle and v its instantaneous velocity.

For a practical quadrupole, the field gradient g varies along the z-axis as shown by the solid line of Fig. 2. For purposes of computation, a "hard-edge model" (Steffen, 1964) is used, as shown by the dashed line of Fig. 2. Consequently one defines an "effective length" L such that

$$L = \frac{\int_{-\infty}^{+\infty} g(z)dz}{g} \qquad (2.2.4)$$

where g(z) is the measured field gradient along the z-axis of the real quadrupole and g is the value of the gradient well inside the magnet. This definition of L ensures that the actual field and the hard-edge model field are equivalent to first order of approximation in so far as their focussing (or defocussing) action on a charged particle is the same.

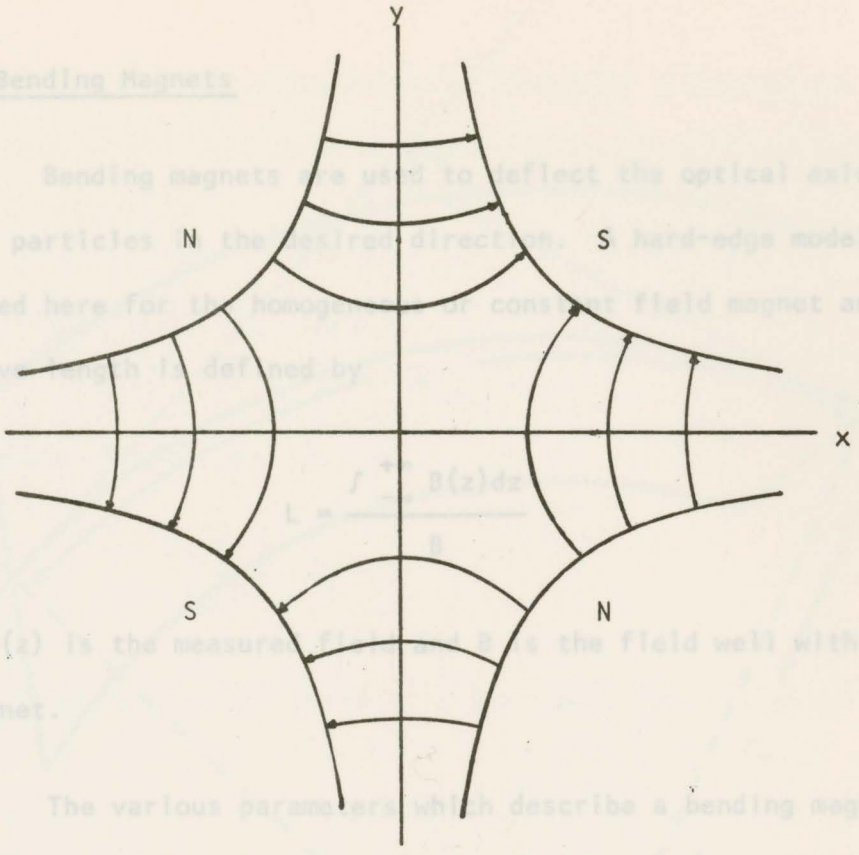

Fig. 1 The Ideal Quadrupole Field

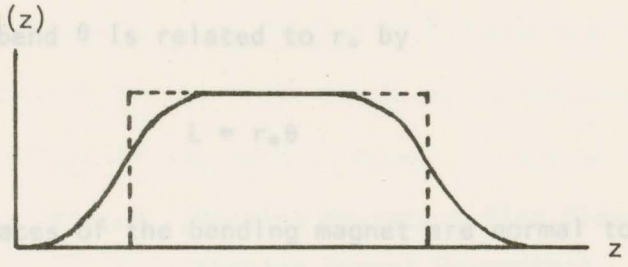

Fig. 2 The Hard-Edge Model

2.2.2 Bending Magnets

Bending magnets are used to deflect the optical axis of a beam of particles in the desired direction. A hard-edge model is also used here for the homogeneous or constant field magnet and the effective length is defined by

$$L = \frac{\int_{-\infty}^{+\infty} B(z)dz}{B} \tag{2.2.5}$$

where $B(z)$ is the measured field and B is the field well within the magnet.

The various parameters which describe a bending magnet are indicated in Fig. 3. The magnetic field is related to the radius of curvature, r_o, and the magnetic rigidity $(B\rho)$ by

$$B = \frac{(B\rho)}{r_o} \tag{2.2.6}$$

The angle of bend θ is related to r_o by

$$L = r_o\theta \tag{2.2.7}$$

If the pole faces of the bending magnet are normal to the beam axis, the entrance angle ϕ_1 and the exit angle ϕ_2 will each have a value of zero.

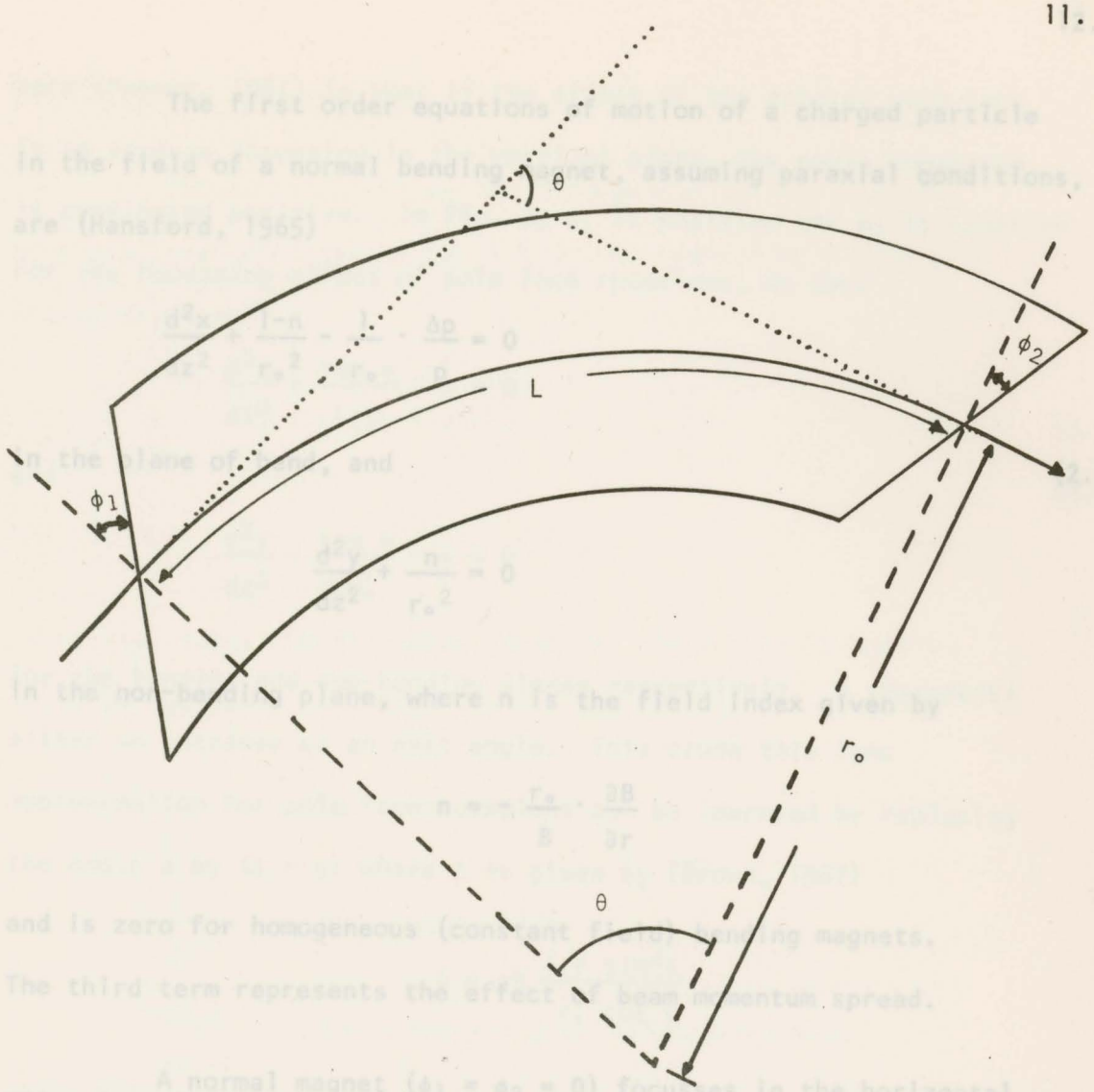

Fig. 3 Bending Magnet, A Plan View
Showing Magnet Parameters

The first order equations of motion of a charged particle in the field of a normal bending magnet, assuming paraxial conditions, are (Hansford, 1965)

$$\frac{d^2x}{dz^2} + \frac{1-n}{r_o^2} - \frac{1}{r_o} \cdot \frac{\Delta p}{p} = 0$$

in the plane of bend, and (2.2.8)

$$\frac{d^2y}{dz^2} + \frac{n}{r_o^2} = 0$$

in the non-bending plane, where n is the field index given by

$$n = - \frac{r_o}{B} \cdot \frac{\partial B}{\partial r}$$

and is zero for homogeneous (constant field) bending magnets. The third term represents the effect of beam momentum spread.

A normal magnet ($\phi_1 = \phi_2 = 0$) focusses in the horizontal plane. A bending magnet with rotated pole faces has additional focussing properties on the edges which may strengthen or weaken the focussing effect of the normal magnet; it can be considered as a normal magnet and each of the pole face rotations can be represented by a thin lens or, as it is often called, a focussing (or defocussing) edge. Whether the thin lens is a focussing or a defocussing edge depends on the sign of the angles ϕ_1 and ϕ_2. The convention used

here (Penner, 1961) is that if the effect of the rotated pole face is to produce focussing in the vertical plane, the angle concerned is considered positive. In Fig. 3, ϕ_1 is positive and ϕ_2 is negative. For the focussing effect of pole face rotations, we have

$$\frac{d^2x}{dz^2} + \frac{\tan \phi}{Lr_o} \cdot x = 0$$

and (2.2.9)

$$\frac{d^2y}{dz^2} - \frac{\tan \phi}{Lr_o} \cdot y = 0$$

for the bending and non-bending planes respectively. ϕ represents either an entrance or an exit angle. This crude thin lens approximation for pole face rotations can be improved by replacing the angle ϕ by $(\phi - \psi)$ where ψ is given by (Brown, 1967)

$$\psi = ah \frac{1 + \sin^2\phi}{r_o \cos \phi}$$

where h is the magnet gap and a is evaluated for the fringing fields. Typical values of a for actual magnet may range from 0.3 to 1.0 depending on the geometry of the magnet. For the purpose of computation a value of 0.5 or 0.6 may be taken.

2.3 Particle Trajectories

The equations of motion through the various elements of a beam transport system can all be represented by a single trajectory equation.

$$\frac{d^2u}{dz^2} + k(z)u - d = 0 \qquad (2.3.1)$$

$$u = x \text{ or } y$$

where k(z) takes the following forms for the various elements given by equations (2.2.3), (2.2.8), and (2.2.9):

$\frac{1}{Lf}$ for a thin lens

$\frac{g}{(B\rho)}$ for a quadrupole

$\frac{\tan \phi}{Lr_o}$ for a focussing or defocussing edge

$\frac{1-n}{r_o^2}$ for a bending magnet in the plane of bend

$\frac{n}{r_o^2}$ for bending magnet in the non-bending plane

and d has the form.

$\frac{1}{r_o} \cdot \frac{\Delta p}{p}$ in the plane of bend for a beam of particles with momentum spread.

The solutions to the linearised equation (2.3.1) are given in terms of the trigonometric sine and cosine functions when the element is focussing, $k(z) > 0$, and in terms of the hyperbolic functions when defocussing, $k(z) < 0$.

In matrix notation (Penner, 1961), the solutions can be represented by

$$\begin{pmatrix} u \\ u' \\ \frac{\Delta p}{p} \end{pmatrix} = \begin{pmatrix} T_{11} & T_{12} & T_{13} \\ T_{21} & T_{22} & T_{23} \\ 0 & 0 & 1 \end{pmatrix} \begin{pmatrix} u_o \\ u'_o \\ \frac{\Delta p}{p} \end{pmatrix} \qquad (2.3.2)$$

where $u = x$ or y and the zero subscript refers to initial values of the displacement u, the slope $u' = \frac{du}{dz}$ and the momentum deviation $\frac{\Delta p}{p}$ which is constant. The matrix elements T_{ij} are functions of the trigonometric circular or hyperbolic sine and cosine functions.

When $u_o = 0$, $u'_o = 1$ and $\frac{\Delta p}{p} = 0$, u is called a sine-like trajectory.

When $u'_o = 0$, $u_o = 1$ and $\frac{\Delta p}{p} = 0$, u is called a cosine-like trajectory.

When $u_o = u'_o = 0$ and $\frac{\Delta p}{p} = 1$, u is called a dispersion trajectory.

The above three trajectories are called "principle trajectories"; all other trajectories can be expressed in terms of these principal trajectories. If the displacement and slope of the output trajectories after the final element are independent of the beam momentum, the system is called "dispersionless" or "achromatic". For such a system, the T_{13} and T_{23} components of the transfer matrix are zero.

2.4 Beam Envelopes

2.4.1 Phase Space

Phase space is the six dimensional space (x, y, z, p_x, p_y, p_z) where x, y, and z are the position coordinates in three dimensional Cartesian space and p_x, p_y, and p_z are the three corresponding momentum coordinates for a point in this space. The motion of a particle in time in the three-dimensional position space is represented by the motion of a point in phase space; and a beam of particles is represented by a group of points in phase space, each point corresponding to one particle in the beam. The group of points will then fill a certain volume in phase space; the surface of this volume defines the boundaries of the beam.

On transformation of the phase space volume in time, the particle density in phase space obeys Liouville's Theorem.

2.4.2 Liouville's Theorem

This theorem states that for motion in an external field, for which Hamiltonian equations can be written, the particle density in phase space remains constant. Thus the phase space volume containing a group of particles remains constant although the shape may change. A derivation of this theorem is given in Steffen (1964).

If the particle motion along the three coordinates of real space is mutually independent, the theorem applies to the motion in each plane separately and the areas in the three hyper-planes (x, p_x), (y, p_y), and (z, p_z) remain constant. In paraxial beam optics one can assume in the linear approximation that the axial momentum p_z is constant, thus

$$p_x = m \frac{dx}{dt} = m \frac{dx}{dz} \cdot \frac{dz}{dt} = p_z x' \ .$$

Since $x' \alpha p_x$, the area in phase plane (x, x') which is occupied by a beam of particle trajectories is also a constant of the motion. Similarly the area in the phase plane (y, p_y) can be represented by an area in the plane (y, y') and its size remains constant.

2.4.3 Emittance and Acceptance

The area of phase space divided by the constant π containing the trajectories of a beam of particles is called the emittance of the beam. The area in phase space enclosed by all particle trajectories transmitted by a beam handling device is referred to as the acceptance of the device.

2.4.4 Ellipse Representation

The most common phase space contour of beams encountered in practice is a polygon. But this can be well approximated by an ellipse which contains a given fraction of the particle trajectories (e.g. 90% of them). The ellipse representation offers certain advantages; it can be described by three parameters only, it can conveniently be handled mathematically, and more important, it retains its elliptical shape on transforming through a linear beam transport system.

The equation of the phase space ellipse in the (u, u') space is (Steffen, 1964)

$$\gamma u^2 + 2\alpha uu' + \beta u'^2 = \varepsilon \ , \qquad (2.4.1)$$

with the normalizing condition

$$\beta\gamma - \alpha^2 = 1 \ ,$$

where u = x or y.

β is called the amplitude function; it is a function of z and it depends on the initial ellipse parameters β_o, α_o, and ε. Fig. 4 shows the phase space ellipse of area F and its relation to the parameters α, β, γ, and ε.

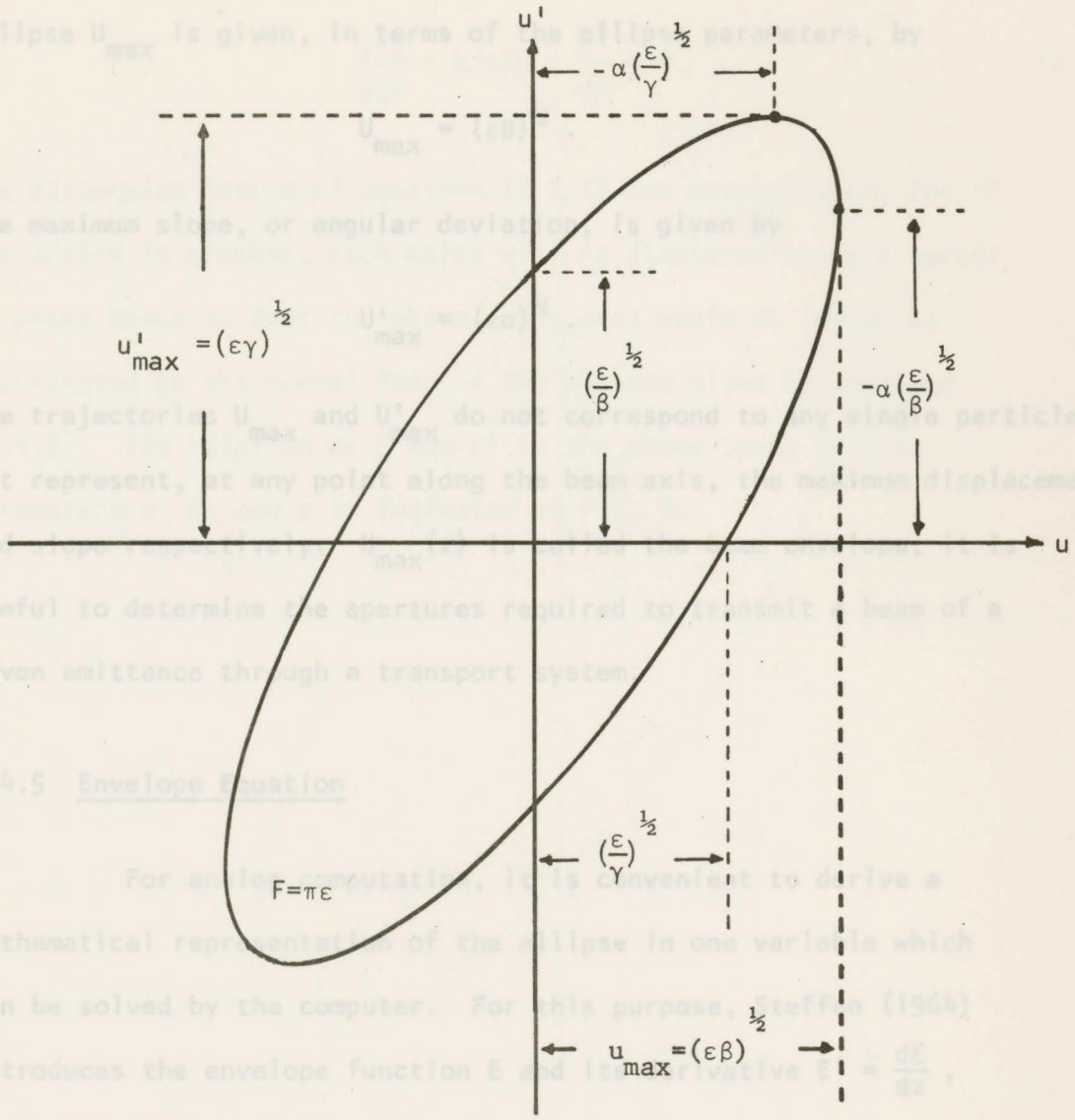

Fig. 4 Phase Space Ellipse, Relation to Ellipse Parameters

The maximum displacement of the trajectories within the ellipse U_{max} is given, in terms of the ellipse parameters, by

$$U_{max} = (\varepsilon\beta)^{\frac{1}{2}} .$$

The maximum slope, or angular deviation, is given by

$$U'_{max} = (\varepsilon\alpha)^{\frac{1}{2}} .$$

The trajectories U_{max} and U'_{max} do not correspond to any single particle but represent, at any point along the beam axis, the maximum displacement and slope respectively. $U_{max}(z)$ is called the beam envelope; it is useful to determine the apertures required to transmit a beam of a given emittance through a transport system.

2.4.5 Envelope Equation

For analog computation, it is convenient to derive a mathematical representation of the ellipse in one variable which can be solved by the computer. For this purpose, Steffen (1964) introduces the envelope function E and its derivative $E' = \frac{dE}{dz}$, which are related to the ellipse parameters by

$$E = (\varepsilon\beta)^{\frac{1}{2}} \quad ; \quad E' = \alpha\left(\frac{\varepsilon}{\beta}\right)^{\frac{1}{2}} .$$

It is seen that $E = U_{max}$; however, $E' \neq U'_{max}$. By substituting for α and β in terms of E and E' in the ellipse equation (2.4.1) and the trajectory equation (2.3.1), it is shown in Appendix A that the

envelope equation is given by

$$\frac{d^2E}{dz^2} + k(z)E - \frac{\varepsilon^2}{E^3} = 0 \ . \qquad (2.4.2)$$

The dispersion term d of equation (2.3.1) was assumed zero, for if dispersion is present, each point will be displaced along a vector in phase space so that the phase space area would no longer be represented by the normal form of the ellipse given by equation (2.4.2). The relation of E and E' to the phase space ellipse parameters α, β, and ε is indicated in Fig. 5.

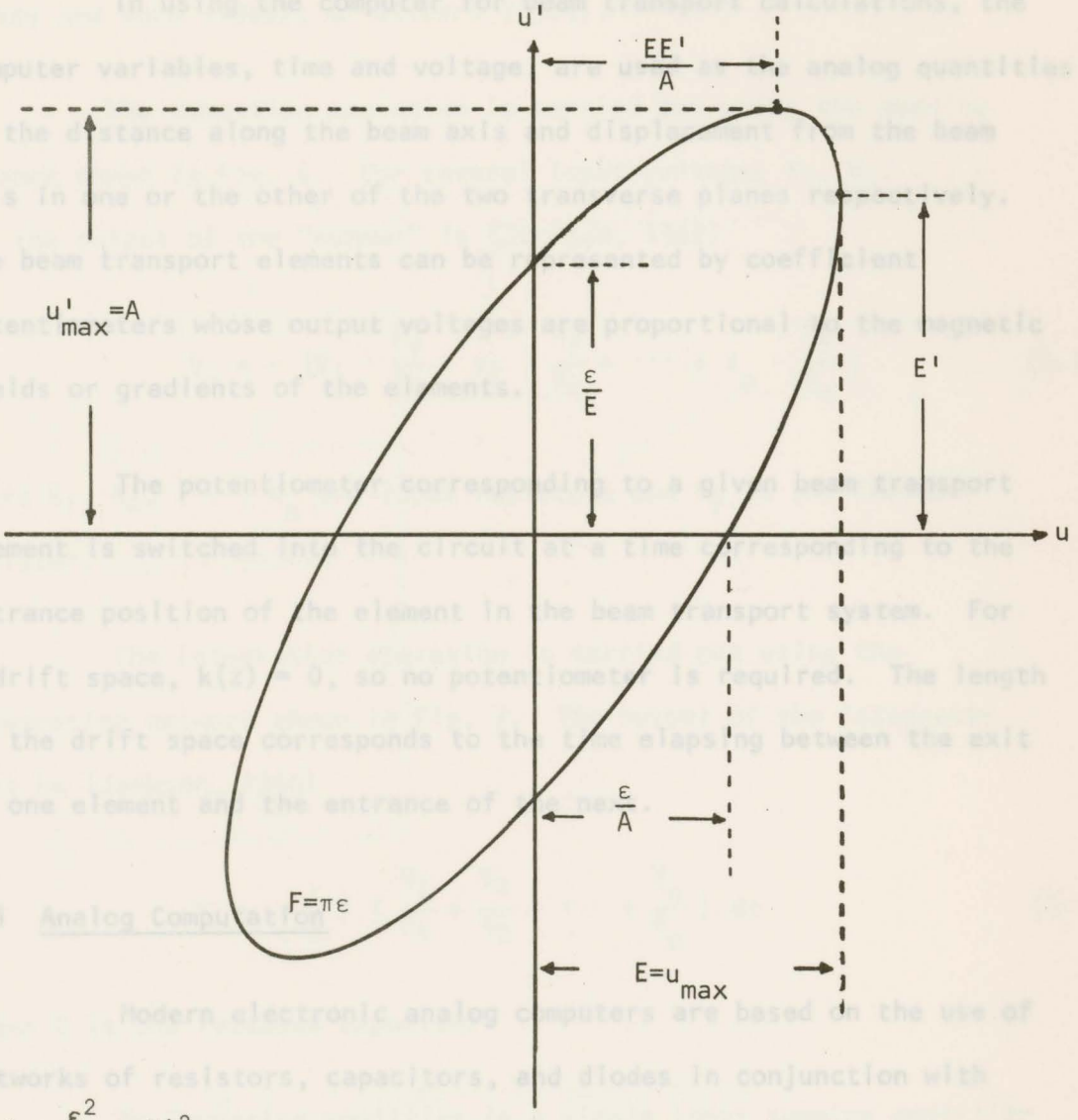

Fig. 5 Phase Space Ellipse, Relation to Envelope Function

3. ANALOG COMPUTATION IN BEAM TRANSPORT SYSTEMS

In using the computer for beam transport calculations, the computer variables, time and voltage, are used as the analog quantities of the distance along the beam axis and displacement from the beam axis in one or the other of the two transverse planes respectively. The beam transport elements can be represented by coefficient potentiometers whose output voltages are proportional to the magnetic fields or gradients of the elements.

The potentiometer corresponding to a given beam transport element is switched into the circuit at a time corresponding to the entrance position of the element in the beam transport system. For a drift space, $k(z) = 0$, so no potentiometer is required. The length of the drift space corresponds to the time elapsing between the exit of one element and the entrance of the next.

3.1 Analog Computation

Modern electronic analog computers are based on the use of networks of resistors, capacitors, and diodes in conjunction with operational amplifiers. The latter are direct-coupled amplifiers with very high gain and input impedance and a low output impedance.

Summation, multiplication, division, integration, and differentiation may be carried out on an analog computer using the operational amplifier. Summation and integration are the two operations required for the solution of the problems encountered

here. Derivation of input-output relations for the latter two operations can be found in Korn and Korn (1956), Jackson (1960), Huskey and Korn (1962), or Gilbert (1964).

The summation operation is carried out using the summing network shown in Fig. 6. For several input voltages V_1, V_2, . . . V_n, the output of the "summer" is (Jackson, 1960)

$$V_o = - \left(V_1 \cdot \frac{R_f}{R_1} + V_2 \cdot \frac{R_f}{R_2} + \cdots + V_n \cdot \frac{R_f}{R_n} \right) \qquad (3.1.1)$$

where R_1, R_2, . . . R_n are input resistors and R_f is the feedback resistor.

The integration operation is carried out using the integrating network shown in Fig. 7. The output of the integrator will be (Jackson, 1960)

$$V_o = - \frac{1}{C} \int \left(\frac{V_1}{R_1} + \frac{V_2}{R_2} + \cdots + \frac{V_n}{R_n} \right) dt \qquad (3.1.2)$$

where C is the feedback capacitor.

An inverting amplifier is a single input summing amplifier with the input and feedback resistors equal.

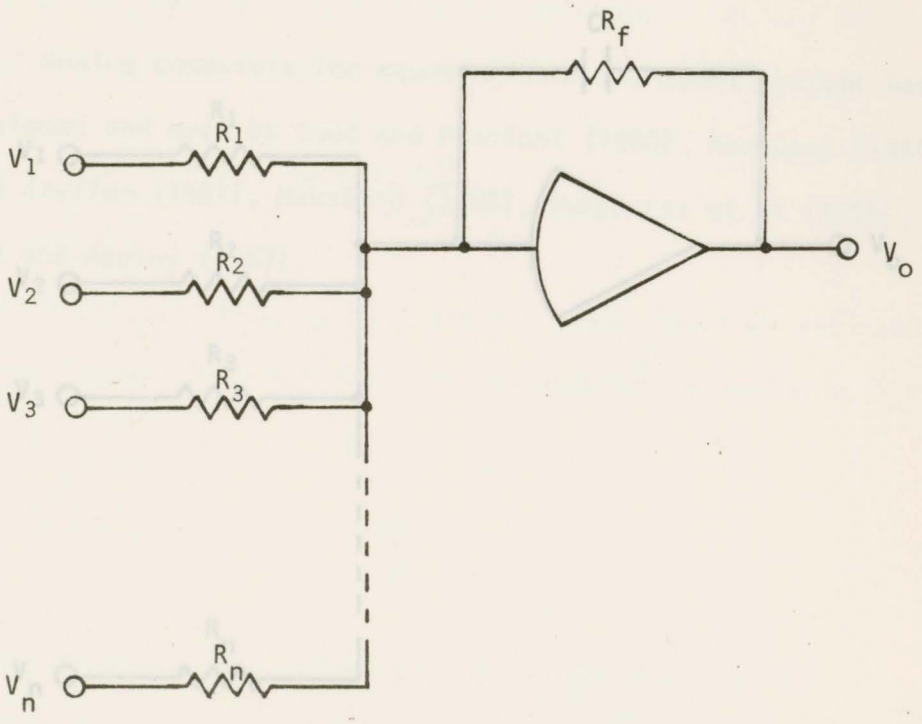

Fig. 6 A Schematic Circuit Diagram
For a Summing Network

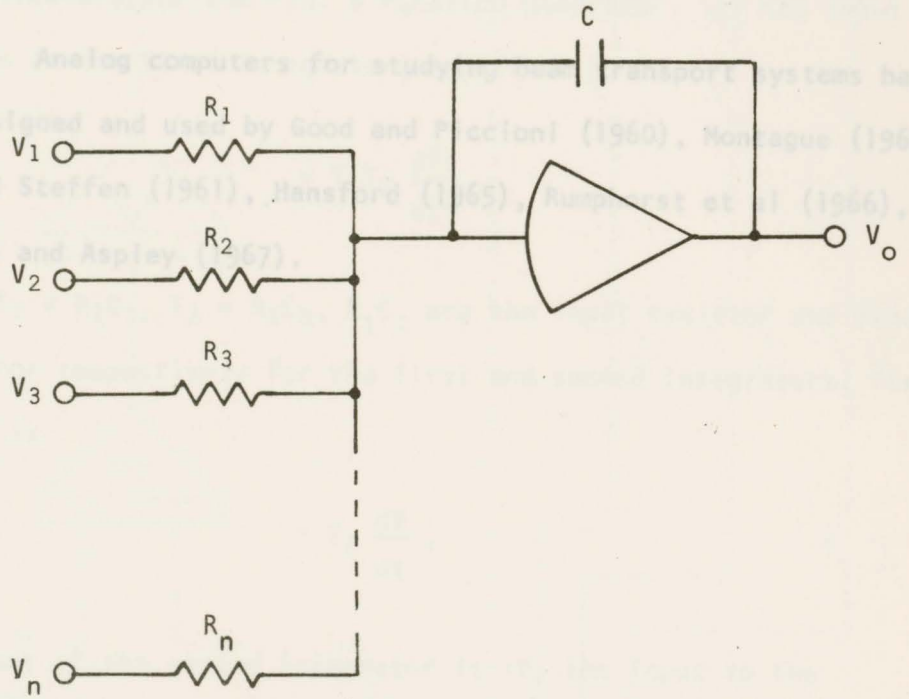

Fig. 7 A Schematic Circuit Diagram
For an Integrating Network

Many equations include a non-linear function, such as the term $\frac{\varepsilon^2}{E^3}$ in equation (2.4.2). For the solution of these equations, non-linear devices are needed to generate the function. Several types of function generators which are in use today are discussed in Section 3.5.

Analog computers for studying beam transport systems have been designed and used by Good and Piccioni (1960), Montague (1960), Kern and Steffen (1961), Hansford (1965), Rumphorst et al (1966), and Hansford and Aspley (1967).

3.2 The Computer Equations

The analog computer solves a set of equations in terms of time and voltage. A description of the system is aided by reference to Fig. 8 where the triangles represent amplifiers, the circles potentiometers, and the F.G. a function generator. If the input voltage to the first integrator, amplifier 5, is

$$+ T_1 T_2 \frac{d^2V}{dt^2} ,$$

where $T_1 = R_1C_1$, $T_2 = R_2C_2$, R_iC_i are the input resistor and feedback capacitor respectively for the first and second integrators, its output is

$$- T_2 \frac{dV}{dt} ,$$

then that of the second integrator is +V, the input to the potentiometers will be -V(+V) when the relay R2 is de-energized (energized) so that the output of a potentiometer f_i is $\pm f_iV$. If this output is introduced into the summing amplifier 3 via the appropriate resistor to produce a gain of A_i, the output of this amplifier will be $\mp A_if_iV$. Therefore, at the input to the first integrator we have

$$T_1 T_2 \frac{d^2V}{dt^2} = \mp A_i f_i V \qquad (3.2.1)$$

or

$$\frac{d^2V}{dt^2} \pm \frac{A_i f_i}{T_1 T_2} V = 0 . \qquad (3.2.2)$$

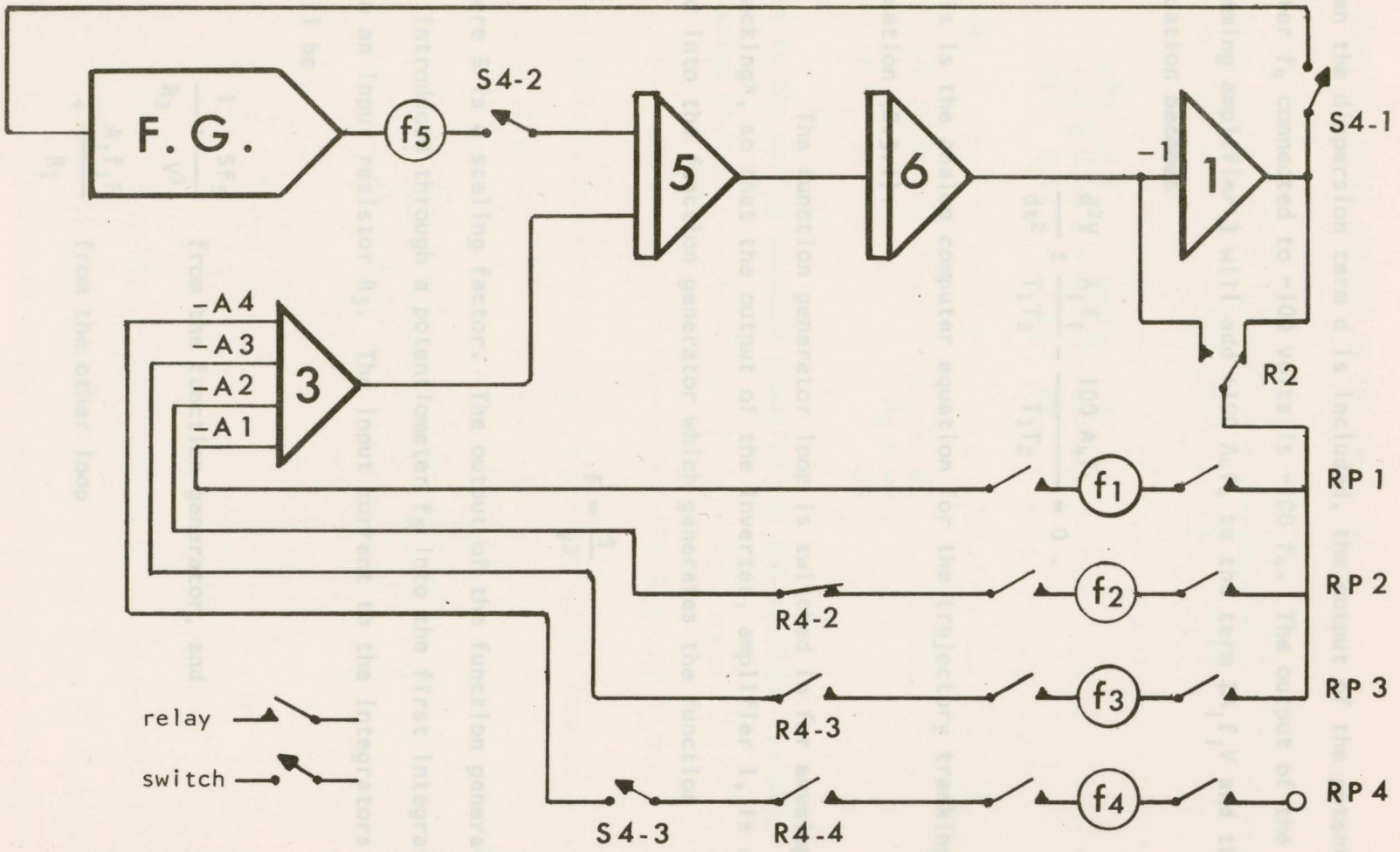

Fig. 8 A Schematic Diagram of the Analog Section

When the dispersion term d is included, the output of the potentiometer f_4 connected to -100 volts is -100 f_4. The output of the summing amplifier 3 will add +100 $A_4 f_4$ to the term $\mp A_i f_i V$ and the equation becomes

$$\frac{d^2V}{dt^2} \pm \frac{A_i f_i}{T_1 T_2} - \frac{100\ A_4 f_4}{T_1 T_2} = 0 \ . \qquad (3.2.3)$$

This is the analog computer equation for the trajectory tracking* equation (2.3.1).

The function generator loop is switched in for envelope tracking*, so that the output of the inverter, amplifier 1, is also fed into the function generator which generates the function

$$F = \frac{S}{V^3}$$

where S is a scaling factor. The output of the function generator is introduced through a potentiometer f_5 into the first integrator via an input resistor R_3. The input current to the integrators will be

$\frac{1}{R_3} \cdot \frac{Sf_5}{V^3}$ from the function generator, and

$\mp \frac{A_i f_i F}{R_1}$ from the other loop

---

* When equations (2.3.1) and (2.4.2) are solved to obtain, at any point in the system, u = u(z) and E = E(z), trajectory tracking and envelope tracking respectively are said to be accomplished.

so that the total current at the input is

$$\frac{T_1T_2}{R_1} \cdot \frac{d^2V}{dt^2} = \mp \frac{A_i f_i V}{R_1} + \frac{Sf_5}{V^3R_3}$$

or

$$\frac{d^2V}{dt^2} \pm \frac{A_i f_i}{T_1T_2} V - \frac{A_5 Sf_5}{T_1T_2} \cdot \frac{1}{V^3} = 0 , \qquad (3.2.4)$$

where

$$A_5 = \frac{R_1}{R_3} .$$

This is the analog computer equation for the envelope tracking equation (2.4.2).

3.3 Scaling

The dependent and independent variables of the computer which must be related to those of the physical problem are voltage and time. The constants used to define the relationships are known as scale factors. For best accuracy the scale factors are chosen, if possible, to use the full dynamic range of the computer. Time t and voltage V in the computer are related to the distance along the beam axis z and the displacement of the trajectory from the beam axis u by

$$z = at$$

and $u = bV$ in the trajectory equation (2.3.1)

or $E = bV$ in the envelope equation (2.4.2).

Substituting these relationships into the computer equations (3.2.3) and (3.2.4) gives

$$\frac{d^2u}{dz^2} \pm \frac{A_i f_i}{a^2 T_1 T_2} \cdot u - \frac{b}{a^2} \cdot \frac{100\, A_4 f_4}{T_1 T_2} = 0 \qquad (3.3.1)$$

and

$$\frac{d^2E}{dz^2} \pm \frac{A_i f_i}{a^2 T_1 T_2} \cdot E - \frac{b^4}{a^2} \cdot \frac{A_5 f_5 S}{T_1 T_2} \cdot \frac{1}{E^3} = 0 \qquad (3.3.2)$$

respectively. Equating the coefficients in the above equations to those in the corresponding beam transport equations, (2.3.1) and (2.4.2), gives the relationships between the computer parameters and the beam transport system parameters

$$k(z) = \pm \frac{A_i f_i}{a^2 T_1 T_2} ,$$

$$d = \frac{b}{a^2} \frac{100\, A_4 f_4}{T_1 T_2} , \qquad (3.3.3)$$

and

$$\varepsilon^2 = \frac{b^4}{a^2} \frac{A_5 f_5 S}{T_1 T_2} .$$

The actual values chosen for a and b depend on the range of magnitudes of the problem variables. The values that have been used in the problems described here are

$a_s = 10^2$ cm. per sec. in the slow mode,

$a_f = 10^3$ cm. per sec. in the fast mode,

and $b = 10^{-1}$ cm. per volt.

From equations (3.3.1), it can be seen that for trajectory tracking without the dispersion term, voltage and time scaling are independent.

3.4 Description of the Computing System

3.4.1 Analog Section

A schematic diagram of the analog circuit is shown in Fig. 8. It consists of two loops; the switch S4 connects the function generator loop into the circuit for the envelope tracking mode and is left open for trajectory tracking. The trajectory tracking loop consists of the two integrators, amplifiers 5 and 6, one inverter, amplifier 1, and a summing amplifier, amplifier 3. The other amplifiers which were used as inverters in the system set up by Louis (1967) were removed from the main loop and used in the function generator unit. Their function is performed by a specially connected relay as shown in Appendix B.

RP1 to RP4 are combinations of relays and potentiometers used for generating the analog to k(z) to simulate the various types of beam transport elements. RP1 consists of a relay combined with the coefficient potentiometer f_1; if the element to be simulated is a quadrupole then the voltage output of f_1 will be set proportional to the magnetic field gradient of the quadrupole.

Combinations like RP1 will simulate quadrupoles and thin lenses (including a focussing or defocussing edge of a bending magnet). This type of element contributes in both the (x,z) and (y,z) planes and therefore they are connected directly to the input of the summing amplifier. If the element is focussing, k(z) > 0, R2 is energized simultaneously with RP1.

Bending magnets in the non-bending plane (often defined as the y-plane) are simulated by combinations like RP2. The RP3 type simulates the bending magnets in the plane of bend (the x-plane). If a dispersion term is present, it is simulated by RP4, which is connected in simultaneously with RP3 since dispersion occurs in the plane of bend only.

The multipole relay R4 determines whether the computation is to be carried out in the x- or y-plane. The relay contacts are shown for computation in the y-plane, R4-2 is closed and R4-3 and R4-4 open. In the x-plane, Relay R4 connects in types RP3 and RP4. The relay R4 is controlled by a function switch, not shown in the diagram, by which one or the other of the two planes or alternately both of them are chosen.

3.4.2 The Timing System

The timing system remains unchanged from that described by Louis (1967) except for the addition of a clock control switch. The timing system is illustrated in Fig. 9. Pulses from the three decade clock trigger an AND gate setting a flip-flop on, which, through a relay driver, connects the potentiometer corresponding to a given element into the circuit for a period corresponding to the effective length of the element. The potentiometer is disconnected by a second set of pulses resetting the flip-flop off.

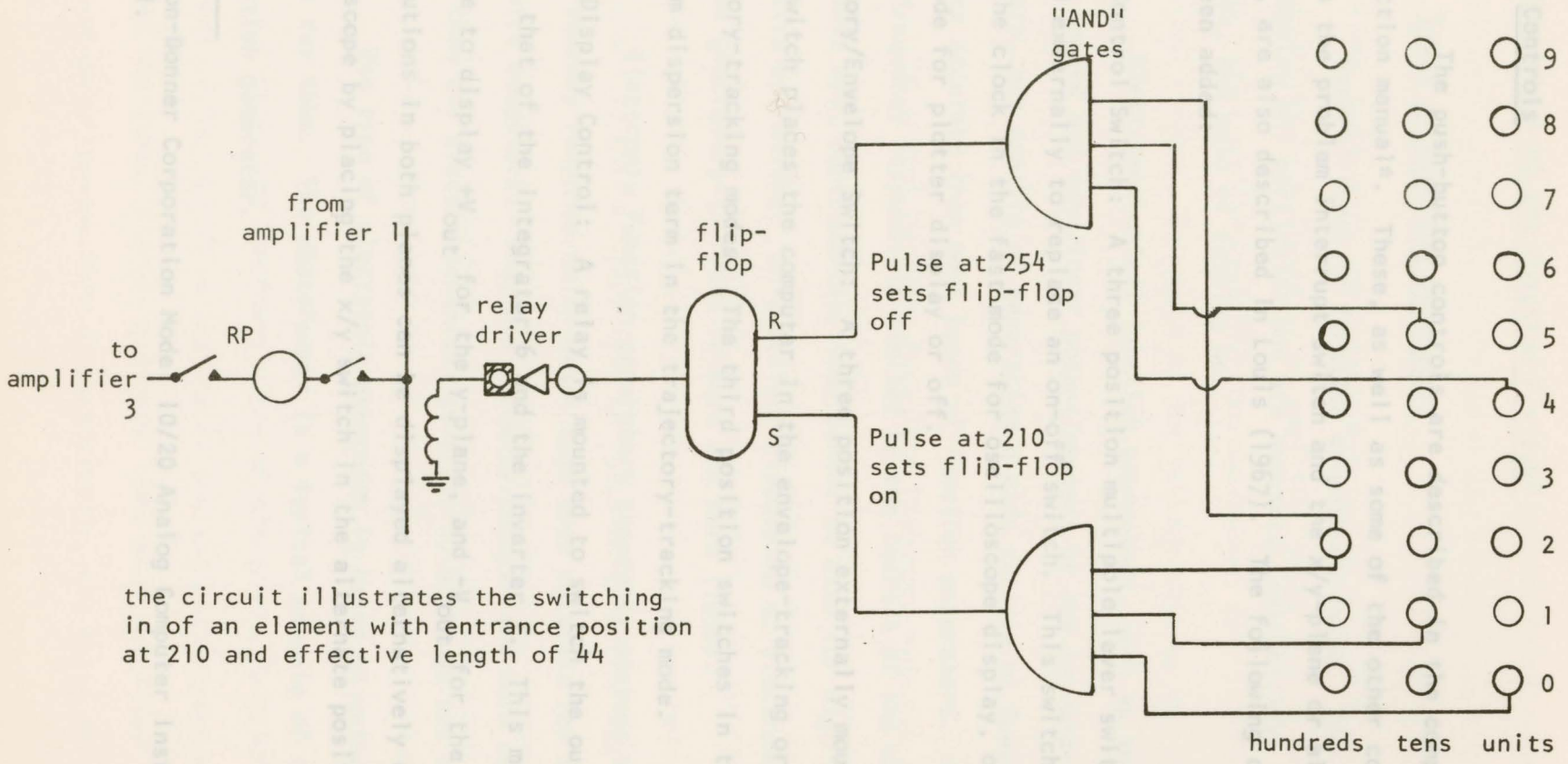

the circuit illustrates the switching in of an element with entrance position at 210 and effective length of 44

Fig. 9 The Timing System

3.4.3 Controls

The push-button controls are described in the computer instruction manual*. These, as well as some of the other controls, such as the problem interrupt switch and the x/y-plane or alternate switch, are also described in Louis (1967). The following controls have been added:

Clock Control Switch: A three position multipole lever switch is mounted externally to replace an on-off switch. This switch can place the clock in the fast mode for oscilloscope display, or in the slow mode for plotter display or off.

Trajectory/Envelope Switch: A three position externally mounted lever switch places the computer in the envelope-tracking or trajectory-tracking modes. The third position switches in the momentum dispersion term in the trajectory-tracking mode.

Output Display Control: A relay is mounted to switch the output between that of the integrator 6 and the inverter 1. This makes it possible to display $+V_{out}$ for the y-plane, and $-V_{out}$ for the x-plane. The solutions in both planes can be displayed alternatively on an oscilloscope by placing the x/y switch in the alternate position.

---

* Systron-Donner Corporation Model 10/20 Analog Computer Instruction manual.

3.5 Generation of the Function $F = S/E^3$

3.5.1 Types of Function Generators

Several types of function generators exist. The criteria for choosing any particular one are accuracy, reliability, frequency response, and ease of setting up.

Electromechanical function generators, such as the servo-driven tapped and non-linear potentiometers or the servo-driven curve followers, are capable of generating a wide variety of functions and are more accurate than most types of function generators. However, their frequency response is limited by the inertia of the mechanical components and, consequently, they cannot be used for high speed repetitive operations. An excellent discussion of electromechanical function generators is found in Korn and Korn (1956).

Electronic function generators generally possess relatively high frequency response which makes them more suitable for fast repetitive computers. They are normally cheaper and more convenient to use than the electromechanical generators, although not as accurate.

One type of electronic generator is based on using the cathode ray tube. The photoformer is a typical example of this class of function generator.

An opaque mask whose profile represents the function to be generated, $y = f(x)$, is fitted on the front of the screen of a cathode ray tube in which the horizontal deflecting voltage represents the independent variable x. The vertical deflection is produced by an amplifier whose input signal is the output of a photomultiplier mounted so that it sees the masked screen. The sense of the voltage causing the vertical deflection is such that the spot on the screen is constrained to move along the edge or profile of the mask and the y-voltage, therefore, represents the function to be generated.

The photoformer has excellent frequency response and is therefore suitable for use with high speed repetitive computers. However, the accuracy is limited by the size of the spot and the size of the face of the cathode ray tube and it deteriorates for very steep slopes. Because of this limitation and the fact that it is rather expensive, this type of function generator was not used.

The most commonly used electronic function generator is the diode function generator, referred to here as the D.F.G. It is reasonably cheap, convenient to use, and particularly suitable for high speed operation. The D.F.G. is discussed in Section 3.5.2.

Finally, an important class of electronic function generators is that based on the use of the voltage-current characteristics of non-linear circuit elements. Not many non-linear elements have accurately reproducible characteristics, but those which do can

be used for generating special function. One type of these elements, which is based on the voltage/current characteristic of semiconductor junctions, is discussed in Section 3.6. It offers a possible alternative to the D.F.G. for generating the function $F = S/E^3$.

3.5.2 The Diode Function Generator

A D.F.G. is an array of resistive networks containing biased diode switches used in conjunction with operational amplifiers to approximate the function to be generated by straight line segments.

The basic element in a D.F.G. is the diode which behaves as a switch that closes (diode conducts) when the input signal exceeds the diode bias voltage. By using several identical diode networks, which will be referred to as segments, with different bias voltages, arbitrary functions may be generated.

To illustrate the principles involved in the form of D.F.G. used in this work, a simple function generator consisting of two segments is shown in Fig. 10, where two switches S_1 and S_2 are used to perform the functions of diodes, and V_{b1} and V_{b2} represent the corresponding bias voltages.

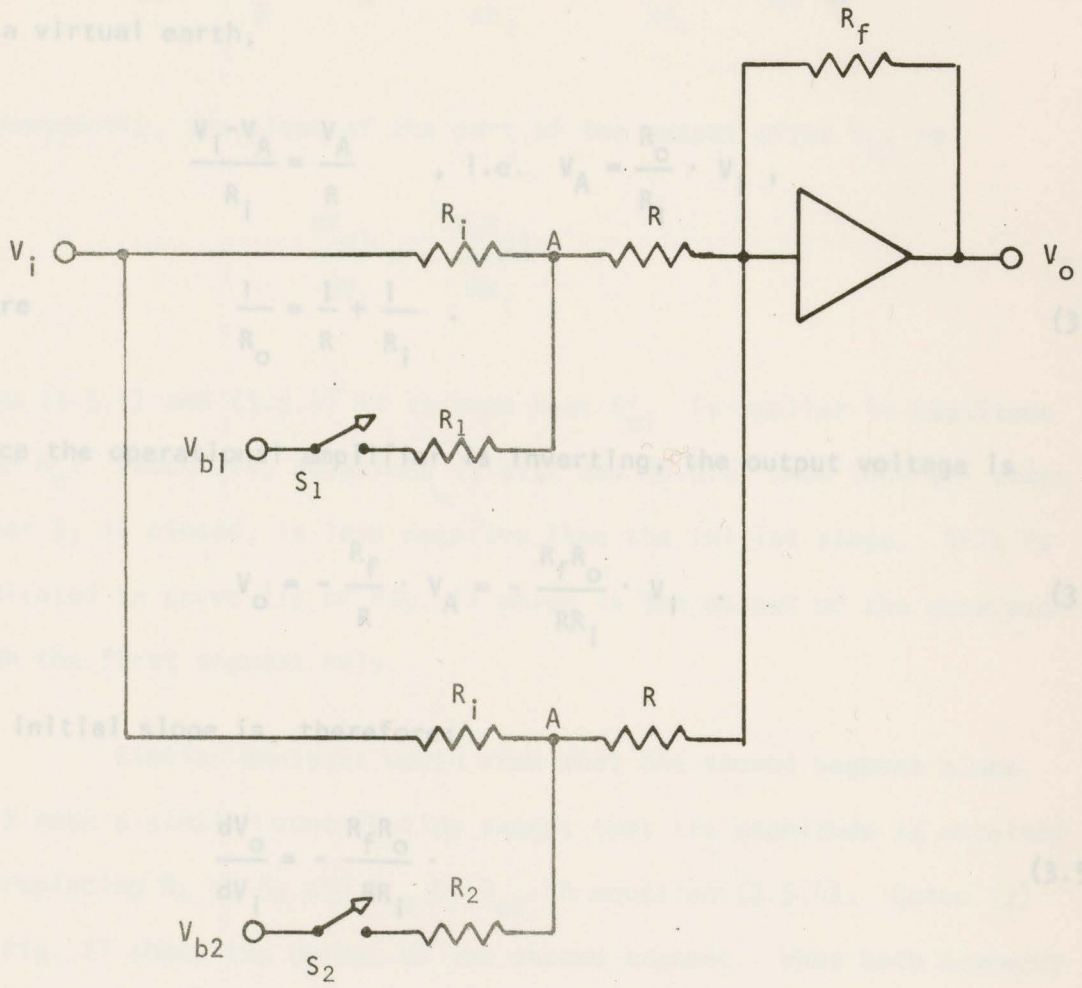

Fig. 10 A Simple Function Generator

Considering the first segment only, when S_1 is open no current will flow through R_1. If the voltage at A is V_A, since VE is a virtual earth,

$$\frac{V_i - V_A}{R_i} = \frac{V_A}{R} \quad , \text{ i.e. } V_A = \frac{R_o}{R_i} \cdot V_i \ ,$$

where

$$\frac{1}{R_o} = \frac{1}{R} + \frac{1}{R_i} \ . \tag{3.5.1}$$

Since the operational amplifier is inverting, the output voltage is

$$V_o = - \frac{R_f}{R} \cdot V_A = - \frac{R_f R_o}{R R_i} \cdot V_i \ . \tag{3.5.2}$$

The initial slope is, therefore:

$$\frac{dV_o}{dV_i} = - \frac{R_f R_o}{R R_i} \ . \tag{3.5.3}$$

When S_1 closes at $V_i = V_{b1}$, some current will flow through R_1. In this case, the voltage at A is given by

$$\frac{V_i - V'_A}{R_i} = \frac{V'_A - V_{b1}}{R_1} + \frac{V'_A}{R}$$

i.e.

$$V'_A = \frac{R_{o1}}{R_i} \cdot V_i + \frac{R_{o1}}{R_i} \cdot V_{b1}$$

with

$$\frac{1}{R_{o1}} = \frac{1}{R} + \frac{1}{R_1} + \frac{1}{R_i} \ . \tag{3.5.4}$$

The output voltage is

$$V'_{o1} = -\frac{R_f}{R} \cdot V'_A = -\frac{R_f R_{o1}}{RR_i} V_i - \frac{R_f R_{o1}}{RR_1} \cdot V_{b1} \qquad (3.5.5)$$

Consequently, the slope of the part of the output after V_{b1} is

$$\frac{dV_{o1}}{dV_i} = -\frac{R_f R_{o1}}{RR_i} . \qquad (3.5.6)$$

From (3.5.1) and (3.5.4) it is seen that R'_{o1} is smaller in magnitude than R_o. Therefore, equations (3.5.3) and (3.5.6) show that the slope after S_1 is closed, is less negative than the initial slope. This is indicated in curve (1) of Fig. 11 which is the output of the generator with the first segment only.

Similar analysis would show that the second segment alone will make a similar contribution except that its magnitude is obtained by replacing R_1 by R_2 and R_{o1} by R_{o2} in equation (3.5.4). Curve (2) of Fig. 11 shows the output of the second segment. When both segments are used with both S_1 and S_2 open, the output V_o contributed by each segment is that given by equation (3.5.2) and the total output is the sum of the two contributions. The initial slope will be

$$\frac{dV_o}{dV_i} = -2\frac{R_f R_o}{RR_i} = -\frac{R_f}{RR_i}(R_o + R_o) \qquad (3.5.7)$$

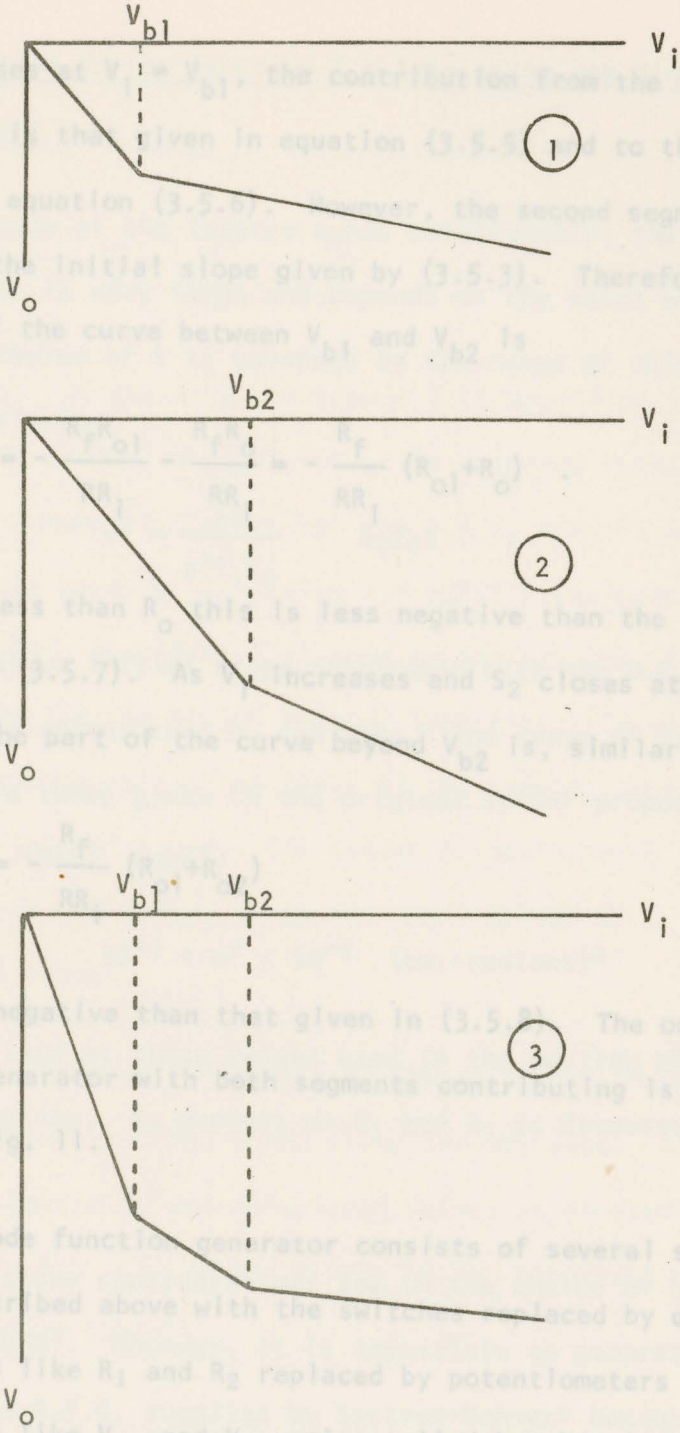

Fig. 11 Output of the Function Generator of Fig. 10

Now if S_1 closes at $V_i = V_{b1}$, the contribution from the first segment to the output is that given in equation (3.5.5) and to the slope is that given in equation (3.5.6). However, the second segment is still contributing the initial slope given by (3.5.3). Therefore, the slope of the part of the curve between V_{b1} and V_{b2} is

$$\frac{dV_o'}{dV_i} = -\frac{R_f R_{o1}}{RR_i} - \frac{R_f R_o}{RR_i} = -\frac{R_f}{RR_i}(R_{o1}+R_o) \quad . \tag{3.5.8}$$

Since R_{o1} is less than R_o this is less negative than the initial slope given in (3.5.7). As V_i increases and S_2 closes at $V_i = V_{b2}$, the slope of the part of the curve beyond V_{b2} is, similarly,

$$\frac{dV_o''}{dV_i} = -\frac{R_f}{RR_i}(R_{o1}+R_{o2}) \tag{3.5.9}$$

which is less negative than that given in (3.5.8). The output of the function generator with both segments contributing is shown in curve (3) of Fig. 11.

A diode function generator consists of several segments like those described above with the switches replaced by diodes, slope resistors like R_1 and R_2 replaced by potentiometers and biasing voltage sources like V_{b1} and V_{b2}, also called break point voltages, are set by potentiomenters from a common voltage supply.

3.5.3 Generation of the Function $F = S/E^3$ Using the Diode Function Generator

Because of the inverse cubic relationship, the initial slope of the function is very large and depends on the value of S to be chosen. The choice of S is governed by the range of values of ε^2 in the scaling relation

$$\varepsilon^2 = \frac{b^4}{a^2 T_1 T_2} \cdot A_5 f_5 S$$

and by the maximum initial slope attainable with the D.F.G. as well as the possible values that A_5 can take. The range of values of ε^2 considered were those given in the original TRIUMF proposal (Vogt and Burgerjon, 1966), namely

$$10^{-9} < \varepsilon^2 < 10^{-5} \quad (\text{cm.-radians})^2$$

a and b were fixed at those values used in the scaling of the trajectory equation. A_5 depends on R_1 and R_3 as discussed in Section 3.2.

The above considerations led to the choice of S = 10 to generate $F = 10/E^3$. However, it is impossible to generate this function on the D.F.G. supplied by Systron-Donner* because of the very high value of the initial slope. The modifications of the D.F.G. to increase the initial slope are discussed in Appendix C.

---

* Systron-Donner Module 3351

With the modified D.F.G. it was possible to generate the function $F = 10^4/E^3$. However, we can write

$$F = \frac{10}{E^3} = \frac{10^4}{(10E)^3} = \frac{10^4}{E'^3}$$

where $E' = 10E$. If the original signal E is amplified by a factor of 10 before it is fed to the D.F.G., the required function will be generated. A schematic diagram for the D.F.G. unit is shown in Fig. 12 with the section generating $F = 10^4/E'^3$ enclosed inside the dotted rectangle. Amplifier 7 is used to amplify the signal E; its output is diode limited to 100 volts. Amplifier 2 is used as an inverter to provide -E' to the input of the summing amplifier 4 for adjusting the initial slope. The output of amplifier 4 is also diode limited to 100 volts, since for small falues of E, the function has very large values.

Fig. 13 shows the output of the unit with the positions of the break point settings shown along the abscissa. The difference D between the generated and calculated values is plotted as a function of the input in Fig. 14. A comparison of the generated and calculated output is given in Table I.

With this function generator, the envelope plots for the two sample problems given in Chapter 5 were produced.

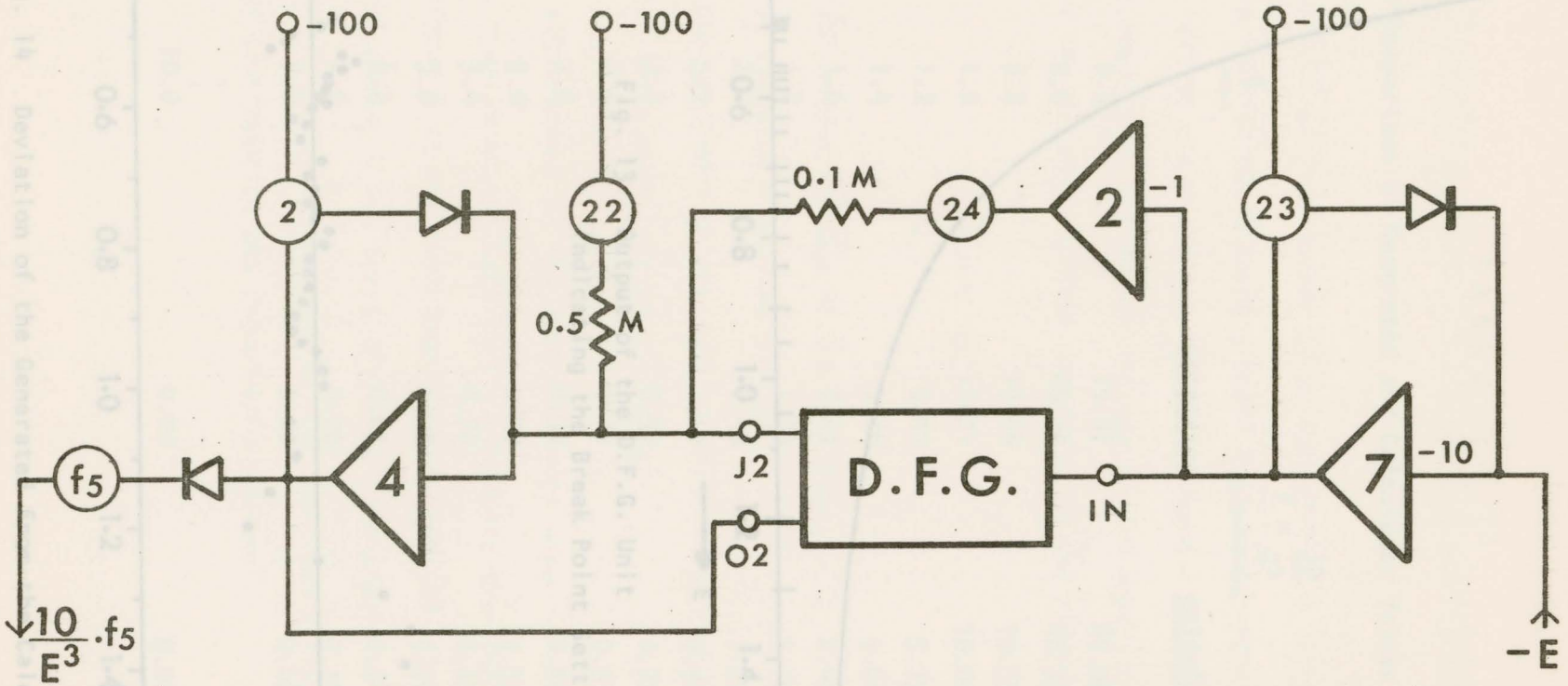

Fig. 12 A Schematic Diagram of the D.F.G. Unit. IN, J2 and 02 are the same as in Fig. C.2

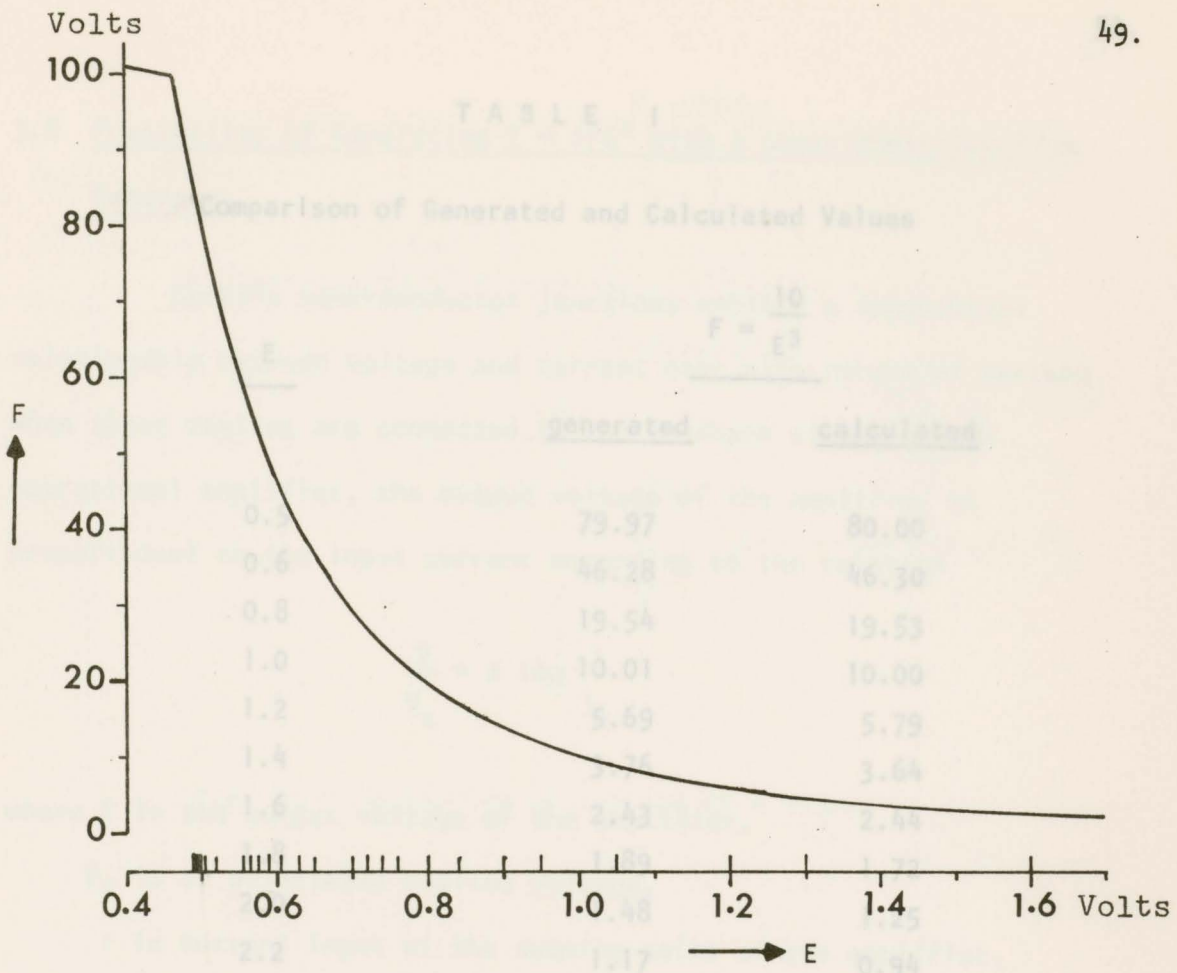

Fig. 13 Output of the D.F.G. Unit
Indicating the Break Point Settings

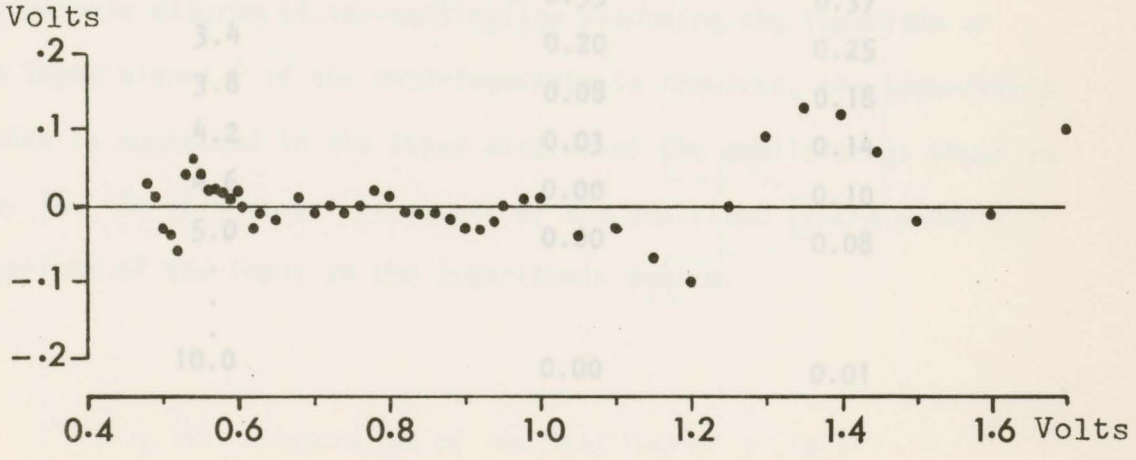

Fig. 14 Deviation of the Generated from the Calculated Values of $F=S/E^3$ as a Function of Input Voltage

TABLE I

Comparison of Generated and Calculated Values

$F = \frac{10}{E^3}$

E	generated	calculated
0.5	79.97	80.00
0.6	46.28	46.30
0.8	19.54	19.53
1.0	10.01	10.00
1.2	5.69	5.79
1.4	3.76	3.64
1.6	2.43	2.44
1.8	1.89	1.72
2.0	1.48	1.25
2.2	1.17	0.94
2.4	0.92	0.72
2.6	0.72	0.57
2.8	0.54	0.46
3.0	0.39	0.37
3.4	0.20	0.25
3.8	0.08	0.18
4.2	0.03	0.14
4.6	0.00	0.10
5.0	0.00	0.08
.		
.		
.		
10.0	0.00	0.01

3.6 Possibility of Generating $F = S/E^3$ with a Logarithmic Function Generator

Certain semi-conductor junctions exhibit a logarithmic relationship between voltage and current over wide ranges of current. When these devices are connected in the feedback circuit of an operational amplifier, the output voltage of the amplifier is proportional to the input current according to the relation

$$\frac{V}{V_s} = \pm \log \frac{I}{I_R}$$

where V is the output voltage of the amplifier,

V_s is an adjustable scaling voltage,

I is current input at the summing point of the amplifier,

and I_R is an adjustable reference current.

The + or - sign depends on the type of device used. Fig 15 shows a schematic diagram of the combination producing the logarithm of the input signal. If the anti-logarithm is required, the logarithmic device is connected in the input circiut of the amplifier as shown in Fig. 16. In this case, the output of the amplifier is the anti-logarithm of the input to the logarithmic device.

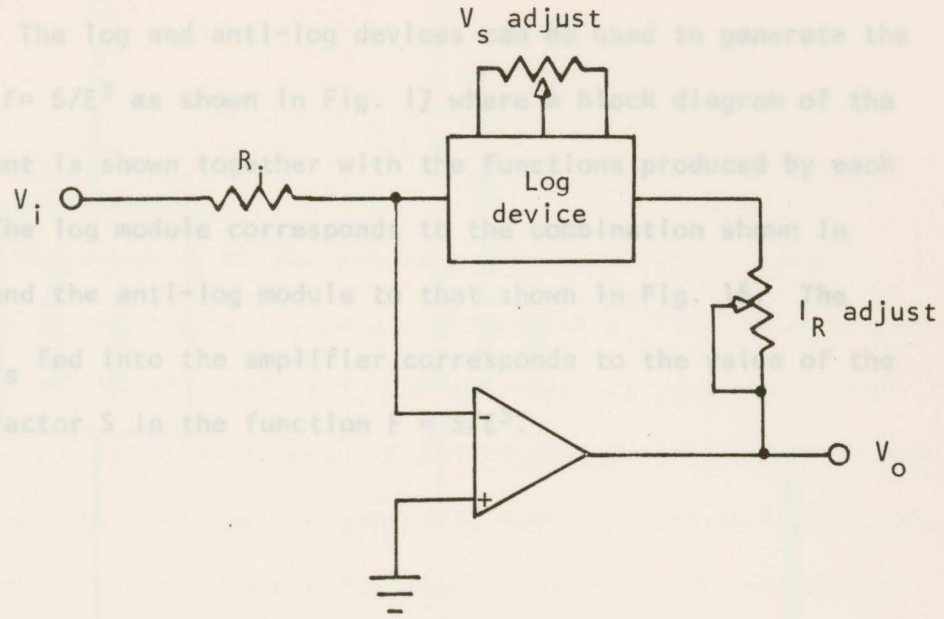

Fig. 15 Generation of the Log of a Signal

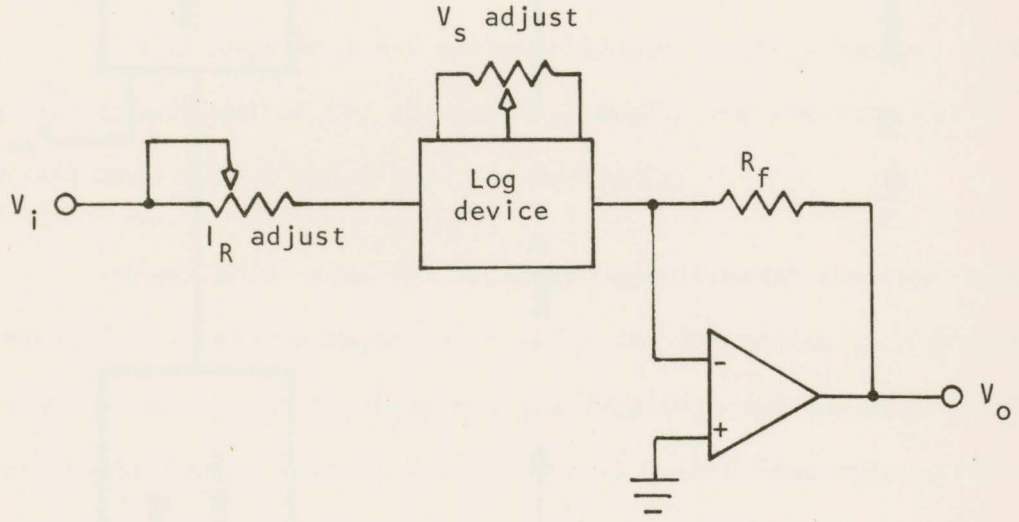

Fig. 16 Generation of the Anti-log of a Signal

The log and anti-log devices can be used to generate the function $F = S/E^3$ as shown in Fig. 17 where a block diagram of the arrangement is shown together with the functions produced by each block. The log module corresponds to the combination shown in Fig. 15 and the anti-log module to that shown in Fig. 16. The voltage E_s fed into the amplifier corresponds to the value of the scaling factor S in the function $F = S/E^3$.

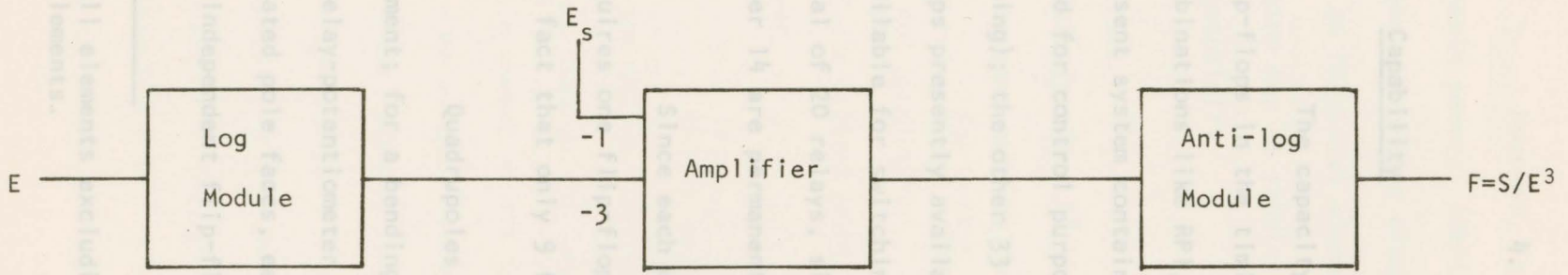

E → - Log E → 3 Log E - Log S → Anti-log (-3 Log E + Log S)
= Anti-log (Log S/E^3)
= S/E^3

Fig. 17 Logarithmic Function Generator

4. CAPABILITY AND ACCURACY

4.1 Capability

The capacity of the system is limited by the number of flip-flops in the timing system and the number of relay-potentiometer combinations like RP1, RP2, RP3, and RP4 that are available. The present system contains a total of 36 AND gates, three of which are used for control purposes (problem interrupt and computer-reset cycle timing); the other 33 are available for switching. Of the 12 flip-flops presently available, 3 are used for logic control so that 9 are available for switching in elements. The relay module contains a total of 20 relays, six of these are used for control purposes, the other 14 are permanently connected to 14 potentiometers.

Since each distinct active element* in the transport system requires one flip-flop for simulation, usually the limiting factor is the fact that only 9 flip-flops are available.

Quadrupoles require one relay-potentiometer combination per element; for a bending magnet with $n \neq 0$ and dispersion term present, 3 relay-potentiometer combinations are required. If the magnet has rotated pole faces, each is represented by a thin lens and requires an independent flip-flop and relay-potentiometer pair.

---

* All elements excluding drift spaces will be referred to as active elements.

However, in so far as most practical beam transport systems contain several identical elements, the computer may handle a larger number of active elements, since one flip-flop may be used to switch in an identical element at a different time. Also, a beam transport system may be subdivided into several sections and tracked sequentially.

The system can be expanded by adding a second flip-flop module in place of the present relay board, which can conveniently be mounted externally since no power supply lines are required for the relay board. This will add 12 more flip-flops for switching purposes.

4.2 Accuracy

The accuracy of an analog system depends partly on the accuracy of the various units and partly on the accuracy with which the analog parameters can be set. The input and feedback resistors and capacitors of the integrating and summing networks have a tolerance of 0.01%. Drift for the integrating network is specified at 100 μV/sec maximum. The noise level for the integrating network was measured at 5 mV r.m.s. and that for the summing network at 12 mV r.m.s.

The errors in setting the potentiometers will contribute to the total error. They are set under problem computing conditions using a digital voltmeter which results in an error not exceeding 10 mV.

Errors in positioning the elements also affect the accuracy of the output. Because of the discrete nature of the 1 kc digital clock output, the length of an element has to be rounded off to a whole number of the unit of length. For active elements, this can be done without introducing significant errors by adjusting k(z) so that the integral $\int k(z)dz$ over the effective length of the element remains constant. This procedure is illustrated in the problem discussed in Section 5.1. For a drift space, k(z) = 0 and such an adjustment is not possible. The rounding off gives rise to an error within $0.5 \times 10^{-3} \times a$ where "a" is the time scale factor. Another source of error in positioning the elements is the relay's time

response resulting in an uncertainty of less than 0.5 milli-second in the timing system. The errors in positioning the elements are particularly large when the trajectory or the envelope crosses the beam axis at a large angle.

In the envelope tracking mode, another source of error is due to the approximation of the function by straight line segments. This error is negligible at small values of the envelope function, E, but for E = 1.5 to 2 volts (15 to 20 volts input to the D.F.G.), the error amounts to 0.25 volts in a D.F.G. output of 2 volts and less. The noise level in the D.F.G. is specified at 0.2 volts.

The accuracy of the analog system results compared to a digital computer results is illustrated by the sample problems considered in Chapter 5. By plotting the values of the absolute errors and the percentage errors against the analog output for the trajectory and envelope tracking modes, the error in the output voltage was found to be within (2.4% ± 0.2 volts) where the constant represents noise in the system.

5. SAMPLE PROBLEMS AND DESIGN OF A SYSTEM

Two sample problems solved on the analog computer will be discussed in order to show its performance. The results are compared with the solution obtained from the digital computer program "TRIUMF" (Tautz, 1968). A design for a pion beam transport system is given to illustrate the use of the analog for design work.

5.1 Trajectory and Envelope Tracking for a 7.5 meter 30° Bending System

This beam transport system is a section of Beam Line I, designed for the TRIUMF project by Tautz (1968), which transports the 500 MeV proton beam extracted from the accelerator to the pion production targets in one of the experimental areas. The following data are used:

Particle	protons
Energy	= 500 (MeV)
Momentum	= 1090.04 (GeV/c)
Magnetic Rigidity ($B\rho$)	= 0.3636×10^7 (Gauss. cm.)

Details of the system and description of the elements are given in Table 2. Because of the discrete nature of the digital clock output, the lengths of the elements are rounded off to whole numbers of centimeters and, consequently, the gradients of quadrupoles and the fields of bending magnets were adjusted so that integrals

T A B L E 2

7.5 meter 30° Bending System, Description of Elements

Element		Original Parameter Values			Adjusted Values		
No.	Type	L	g	B	L	g	B
1	B.M. $n=0$ $\theta=15^{\circ}$ $\phi_1=\phi_2=0$	64.26	-	14.814	64	-	14.874
2	D.S.	30.48	-	-	30	-	-
3	Q-DH.	43.18	-0.5173	-	43	-0.5195	-
4	D.S.	30.48	-	-	31	-	-
5	Q-FH.	43.18	0.3772	-	43	0.3788	-
6	D.S.	132.08	-	-	132	-	-
7	Q-FH.	40.64	0.3986	-	41	0.3951	-
8	D.S.	132.08	-	-	132	-	-
9	Q-FH.	43.18	0.3772	-	43	0.3788	-
10	D.S.	30.48	-	-	31	-	-
11	Q-DH.	43.18	-0.5173	-	43	-0.5195	-
12	D.S.	30.48	-	-	30	-	-
13	B.M. $n=0$ $\theta=15^{\circ}$ $\phi_1=\phi_2=0$	64.26	-	14.814	64	-	14.874

L is the element length, g the quadrupole gradient in Kilogauss per cm., B the field in Kilogauss of the bending magnet. B.M. refers to a bending magnet, D.S. to a drift space, Q-FH. to a horizontally focussing quadrupole and Q-DH. to a horizontally defocussing quadrupole.

$\int g(z)dz$ and $\int B(z)dz$

over the effective length of the elements remained constant. The adjusted values of these parameters are shown in the last three columns of Table 2.

The settings f_i of the coefficient potentiometers corresponding to the various elements are given in Table 3 along with their exit positions along the beam axis. Values of f_i were obtained by using the appropriate expressions for k(z) discussed in Section 2.3, the scaling relations (3.3.3), together with the following values of T_1 and T_2:

$T_1 = 0.1$; $T_2 = 1.0$ for $a_s = 10^2 \frac{(cm.)}{(sec.)}$ in the slow mode,

and $T_1 = 0.01$; $T_2 = 0.1$ for $a_f = 10^3 \frac{(cm.)}{(sec.)}$ in the fast mode.

Fig. 18 shows the resulting trajectories obtained on the xy-plotter in both the horizontal (dashed curves) and vertical planes. Sine-like trajectories, zero initial displacements, and cosine-like trajectories, zero initial slope, are plotted for each plane.

TABLE 3

7.5 meter 30^{o} Bending System, Values Used on the Analog Computer

Elements		exit position along z	f_i	A_i
No.	Type	(cm.)		
1	B.M.	064	0.166	0.1
2	D.S.	094	-	
3	Q-DH.	137	-0.1429	1.0
4	D.S.	168	-	
5	Q-FH.	211	0.1042	1.0
6	D.S.	343	-	
7	Q-FH.	384	0.1087	1.0
8	D.S.	516	-	
9	Q-FH.	559	0.1042	1.0
10	D.S.	590	-	
11	Q-DH.	633	-0.1429	1.0
12	D.S.	663	-	
13	B.M.	727	0.166	0.1

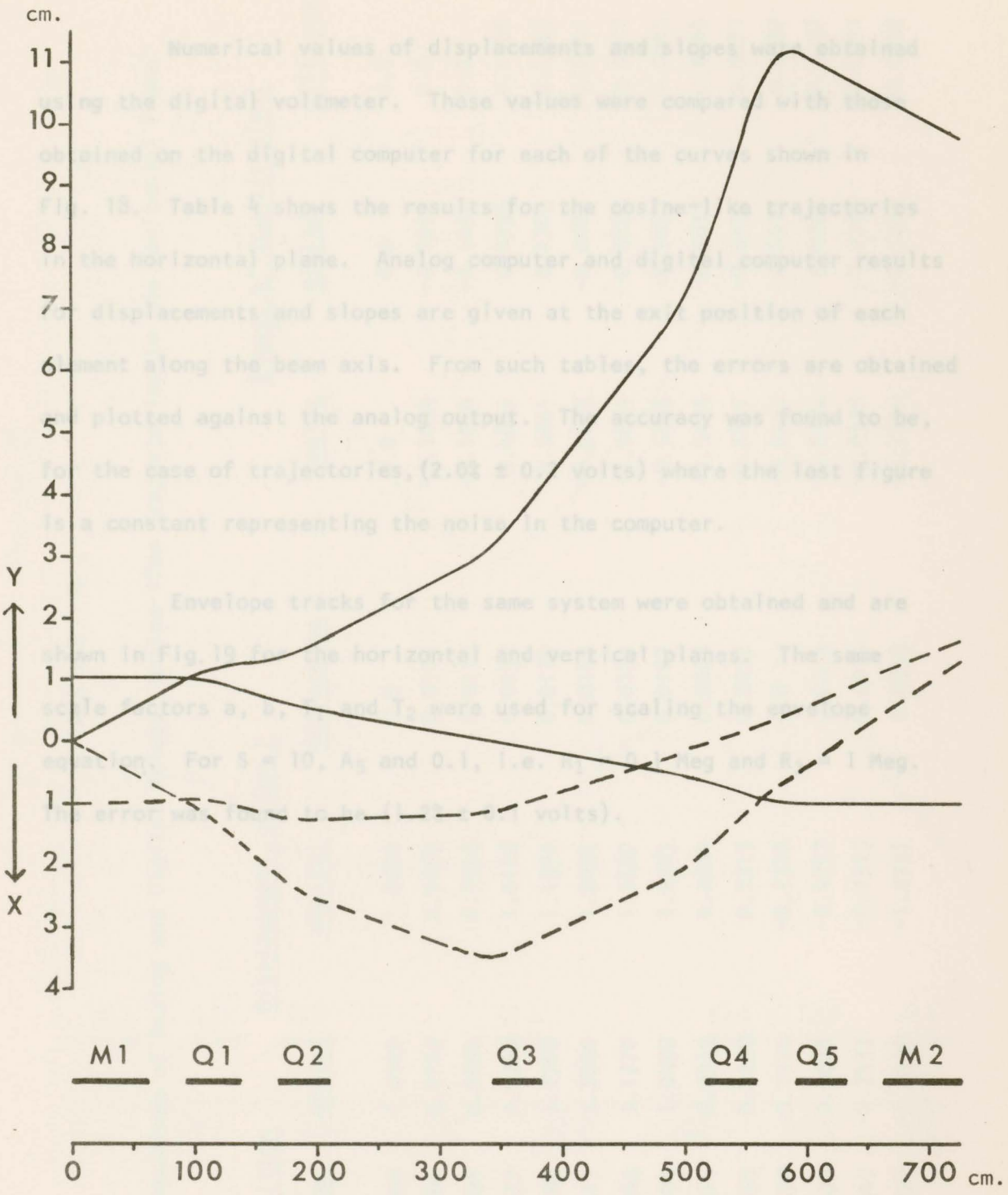

Fig. 18 7.5 meter 30° Bending System, Principal Trajectories in the Horizontal and Vertical Planes

Numerical values of displacements and slopes were obtained using the digital voltmeter. These values were compared with those obtained on the digital computer for each of the curves shown in Fig. 18. Table 4 shows the results for the cosine-like trajectories in the horizontal plane. Analog computer and digital computer results for displacements and slopes are given at the exit position of each element along the beam axis. From such tables, the errors are obtained and plotted against the analog output. The accuracy was found to be, for the case of trajectories, (2.0% ± 0.2 volts) where the last figure is a constant representing the noise in the computer.

Envelope tracks for the same system were obtained and are shown in Fig. 19 for the horizontal and vertical planes. The same scale factors a, b, T_1 and T_2 were used for scaling the envelope equation. For S = 10, A_5 and 0.1, i.e. R_1 = 0.1 Meg and R_3 = 1 Meg. The error was found to be (1.2% ± 0.1 volts).

TABLE 4

Comparison of Analog and Digital Values, Cosine-like Trajectories in the Horizontal Plane

Element	Position	Displacement, x (cm.)			Slope, x' (centiradian)		
No.	cm.	analog	digital	difference	analog	digital	difference
0	000	1.0000	1.0000	0.0	0.0	0.0	0.0
1	064	0.9765	0.9659	0.0106	-0.1054	-0.1054	0.0
2	094	0.9450	0.9338	0.0112	-0.1054	-0.1054	0.0
3	137	1.0260	1.0128	0.0132	0.4861	0.4796	0.0065
4	168	1.1760	1.1590	0.0170	0.4861	0.4769	0.0065
5	211	1.2680	1.2492	0.0188	-0.0685	-0.0686	0.0001
6	343	1.1770	1.1587	0.0183	-0.0684	-0.0686	0.0002
7	384	1.0450	1.0283	0.0167	-0.5695	-0.5632	0.0063
8	516	0.2912	0.2844	0.0068	-0.5695	-0.5632	0.0063
9	559	0.0250	0.0219	0.0031	-0.6417	-0.6330	0.0087
10	590	-0.1710	-0.1710	0.0	-0.6417	-0.6330	0.0087
11	633	-0.4821	-0.4797	0.0024	-0.8376	0.8285	0.0091
12	663	-0.7333	-0.7323	0.0010	-0.8376	-0.8285	0.0091
13	727	-1.2390	-1.2337	0.0053	-0.7324	-0.7231	0.0093

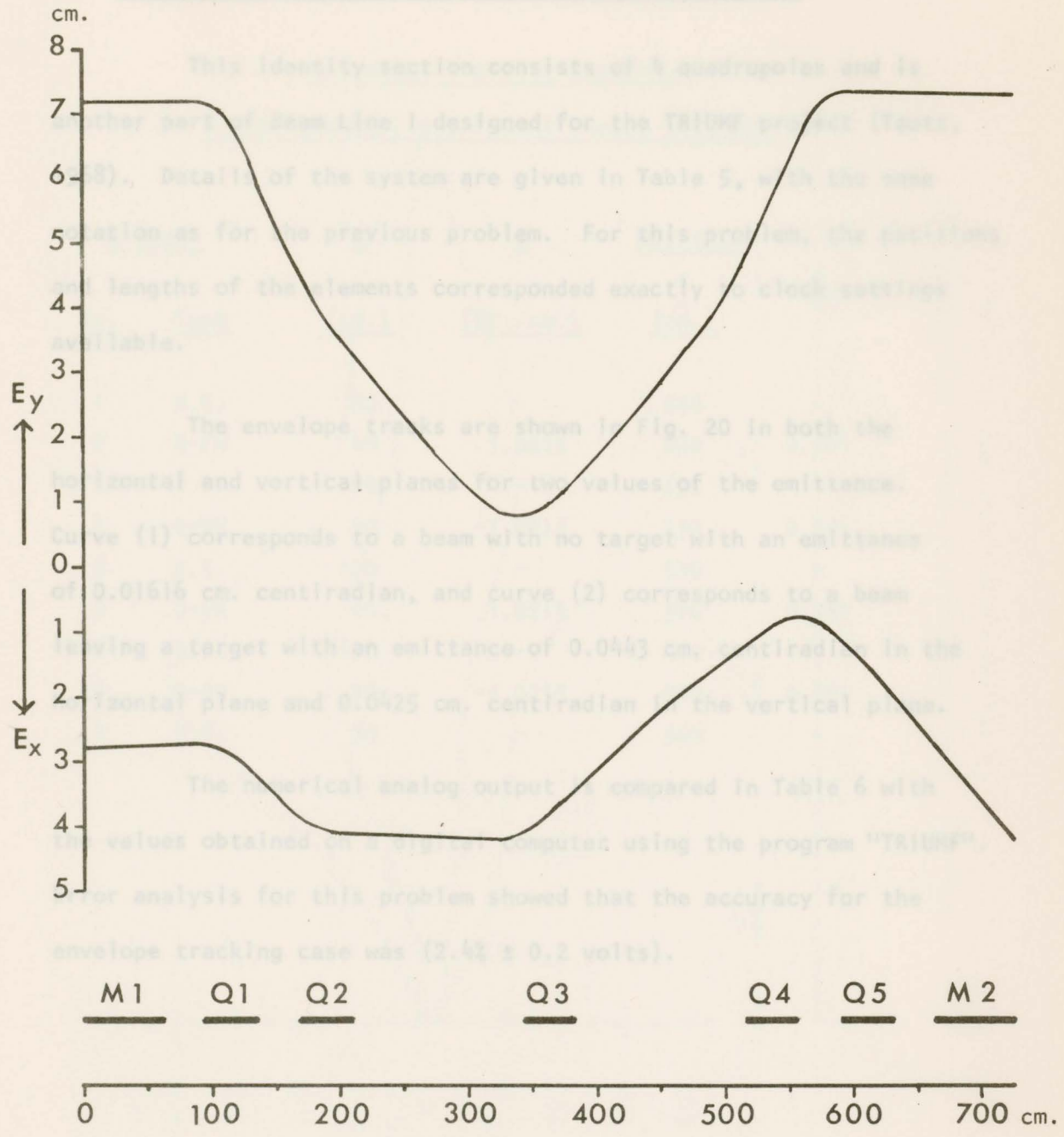

Fig. 19 7.5 meter 30° Bending System, Envelope Tracks in the Horizontal and Vertical Planes

5.2 Envelope Tracking for a 5.6 meter Identity Section

This identity section consists of 4 quadrupoles and is another part of Beam Line I designed for the TRIUMF project (Tautz, 1968). Details of the system are given in Table 5, with the same notation as for the previous problem. For this problem, the positions and lengths of the elements corresponded exactly to clock settings available.

The envelope tracks are shown in Fig. 20 in both the horizontal and vertical planes for two values of the emittance. Curve (1) corresponds to a beam with no target with an emittance of 0.01616 cm. centiradian, and curve (2) corresponds to a beam leaving a target with an emittance of 0.0443 cm. centiradian in the horizontal plane and 0.0425 cm. centiradian in the vertical plane.

The numerical analog output is compared in Table 6 with the values obtained on a digital computer using the program "TRIUMF". Error analysis for this problem showed that the accuracy for the envelope tracking case was (2.4% ± 0.2 volts).

TABLE 5

5.6 meter Identity Section,

Given Parameter and Potentiometer Settings

Element		L	g	Position	
No.	Type	(cm.)	(KG./cm.)	z (cm.)	f_i
1	D.S.	50	-	050	-
2	Q-FH	40	1.0215	090	0.281
3	D.S.	100	-	190	-
4	Q-DH	40	-1.0215	230	0.281
5	D.S.	100	-	330	-
6	Q-FH	40	1.0215	370	0.281
7	D.S.	100	-	470	-
8	Q-DH	40	-1.0215	510	0.281
9	D.S.	50	-	560	-

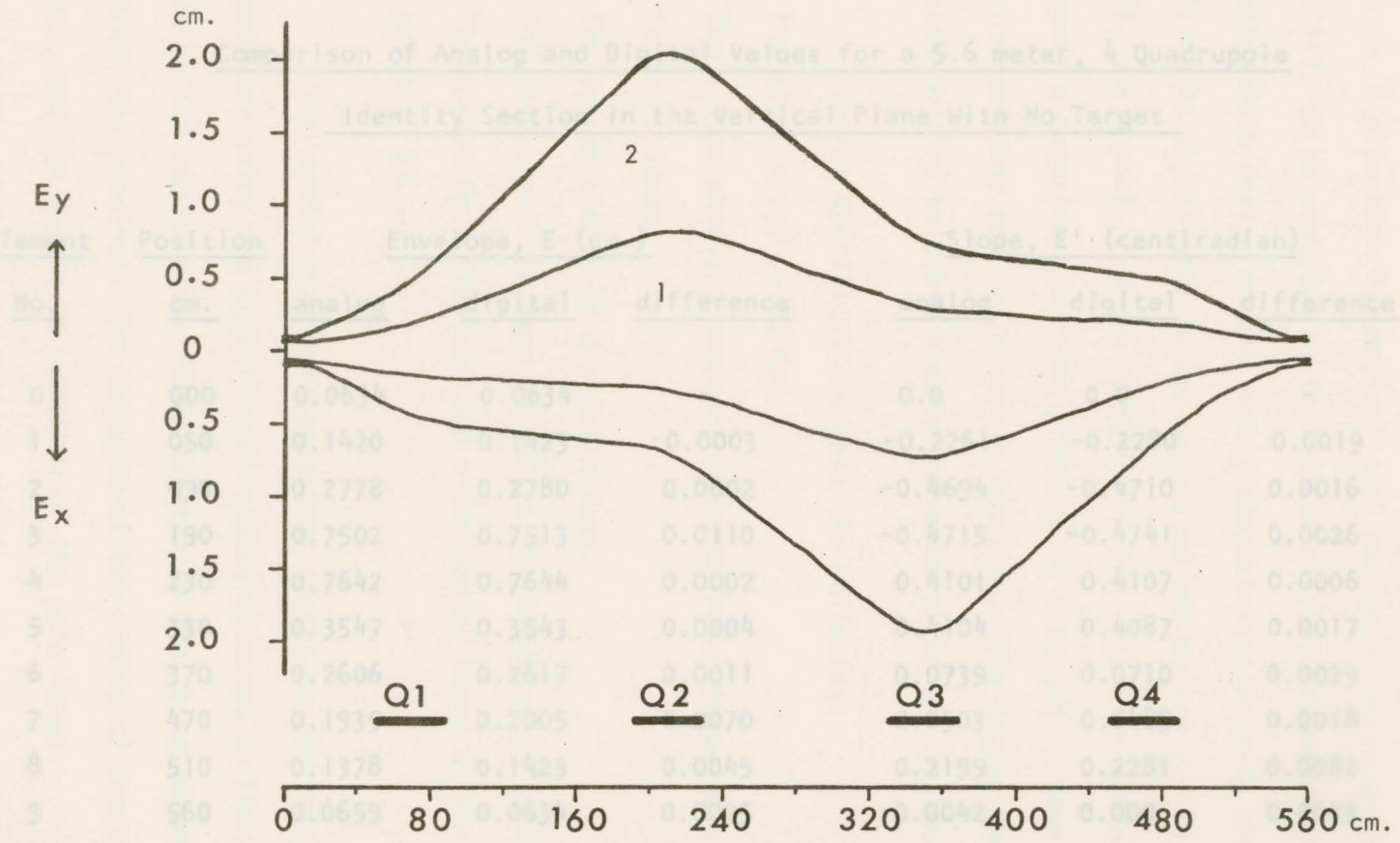

Fig. 20 5.6 meter Identity Section, Envelope Tracks in the Horizontal and Vertical Planes

TABLE 6

Comparison of Analog and Digital Values for a 5.6 meter, 4 Quadrupole Identity Section in the Vertical Plane With No Target

Element	Position	Envelope, E (cm.)			Slope, E' (centiradian)		
No.	cm.	analog	digital	difference	analog	digital	difference
0	000	0.0634	0.0634	-	0.0	0.0	-
1	050	0.1420	0.1423	0.0003	-0.2261	-0.2280	0.0019
2	090	0.2778	0.2780	0.0002	-0.4694	-0.4710	0.0016
3	190	0.7502	0.7513	0.0110	-0.4715	-0.4741	0.0026
4	230	0.7642	0.7644	0.0002	0.4101	0.4107	0.0006
5	330	0.3547	0.3543	0.0004	0.4104	0.4087	0.0017
6	370	0.2606	0.2617	0.0011	0.0739	0.0710	0.0029
7	470	0.1935	0.2005	0.0070	0.0503	0.0485	0.0018
8	510	0.1378	0.1423	0.0045	0.2199	0.2281	0.0082
9	560	0.0659	0.0634	0.0025	0.0042	0.000	0.0042

5.3 Design of a Pion Beam Transport System

A pion beam for medical application is being proposed as a facility to be provided by the TRIUMF project (Batho et al., 1968). An approximate design of the beam transport system using the method of thin lens approximations was suggested and worked out by Lobb (1968), the layout of which is shown in Fig. 21. The system is to transport a negative pion beam produced in a target in Beam Line I to a radiobiology and radiotherapy facility. The analog computer was used to find suitable element parameters for the system.

Design specifications were the following:

(1) The pion energy is 90 MeV.

(2) The system should transform the beam from a focus to a focus in both planes.

(3) The system should be dispersionless.

(4) The beam should be bent by 90° in two bends of 45° each.

(5) There must be a vertical and a horizontal focus at the mid point of Q3.

The method used for design was to set up the system on the computer using the approximate results obtained by Lobb for the values of the parameters. These parameters are the quadrupoles' strengths and spacings, the strength of the fields of the bending magnets, and the angles of rotation of the pole faces.

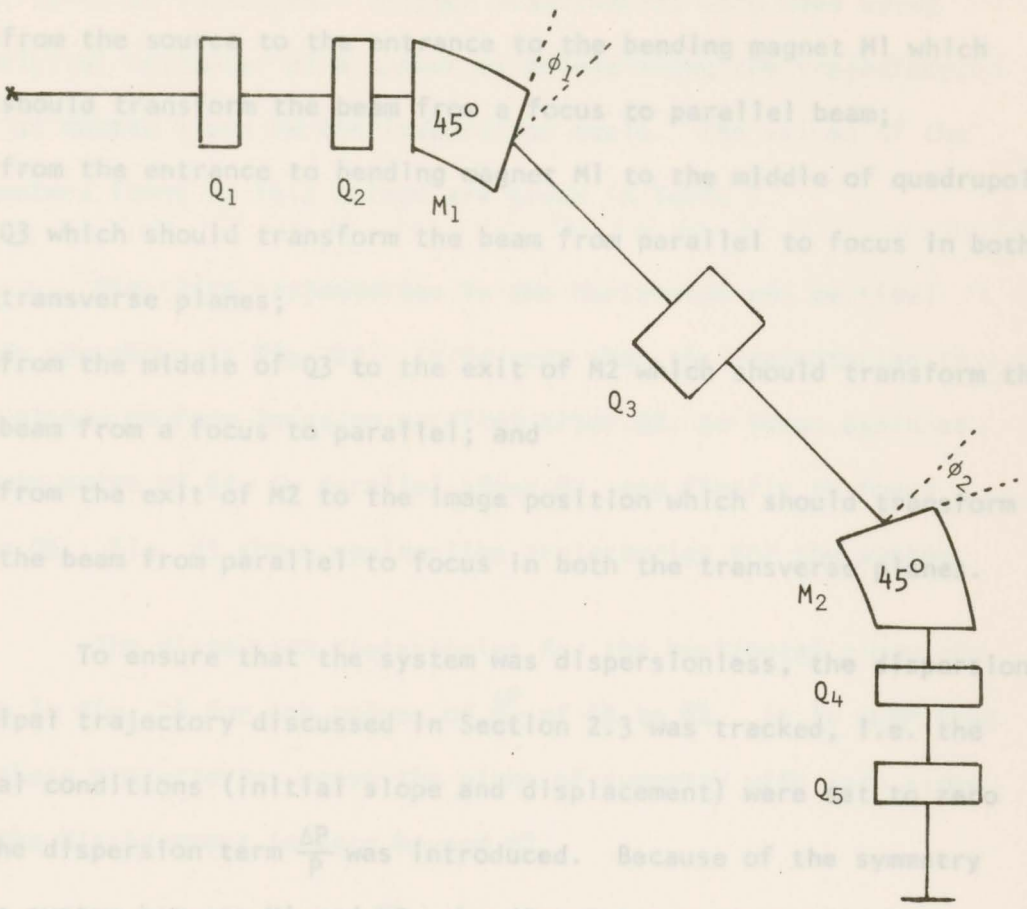

Fig. 21 Layout of the π^- Beam Transport System for Medical Application

For solving the problem, the system was divided into four sections:

(1) from the source to the entrance to the bending magnet M1 which should transform the beam from a focus to parallel beam;

(2) from the entrance to bending magnet M1 to the middle of quadrupole Q3 which should transform the beam from parallel to focus in both transverse planes;

(3) from the middle of Q3 to the exit of M2 which should transform the beam from a focus to parallel; and

(4) from the exit of M2 to the image position which should transform the beam from parallel to focus in both the transverse planes.

To ensure that the system was dispersionless, the dispersion principal trajectory discussed in Section 2.3 was tracked, i.e. the initial conditions (initial slope and displacement) were set to zero and the dispersion term $\frac{\Delta P}{P}$ was introduced. Because of the symmetry of the system between M1 and M2, the dispersion trajectories were made to cross the plane of symmetry at right angles and the displacement was made zero after M2.

Using the thin lens design as a guide, after some adjustments, the spacings between the various elements were chosen and kept fixed. The displacements and slopes, for the trajectories in the cases considered, were displayed on the oscilloscope, while the necessary adjustments of quadrupoles' gradients and fields and rotation angles of bending magnets were made. Records of the final

trajectories were obtained on the xy-plotter and are shown in Figs. 22 to 26 inclusive. Voltage measurements were made using the digital voltmeter at a number of points along the trajectory, i.e. at chosen times in the integration cycle. The values of the parameters found by this method are given in Table 7.

Sine-like trajectories in the horizontal and vertical planes are shown in Fig. 22. It is seen that the trajectories in both planes go from focus to parallel after Q2, to focus again at the mid point of Q3, to parallel after M2, and finally to focus after Q5. Fig. 23 shows cosine-like trajectories for the system.

The dispersion trajectories for the horizontal plane are shown in Fig. 24 for the values of $\frac{\Delta P}{P}$ of 1% to 8%. It is seen that all these trajectories cross the plane of symmetry with zero slope and the displacement is zero beyond M2.

From these principal trajectories, one can determine the components of the transfer matrix at any point in the system. Thus, at the mid-plane, these matrices are

$$\begin{matrix} -0.66 & 0.0 & 1.17 \\ 1.05 & 1.56 & 0.0 \\ 0 & 0 & 1 \end{matrix}$$

in the x-plane, and

$$\begin{matrix} -2.21 & 0.0 & 0 \\ 1.90 & 0.45 & 0 \\ 0 & 0 & 1 \end{matrix}$$

in the y-plane.

From the transfer matrix at the image point, it was found that the magnification in the displacement was 0.634 for the x-plane and 0.609 for the y-plane. The angular magnification was 1.59 and 1.69 for the two planes respectively.

Figs. 25 and 26 show sine-like and cosine-like trajectories respectively in the horizontal planes with values of $\frac{\Delta P}{P}$ from 0 to 7%. These show the effect of the dispersion term on the slope and displacements for the two cases. In both cases, the whole system is dispersionless.

TABLE 7

Parameters Determined for the Pion Bending System

Element No.	Type	z (cm.)	g (G/cm.)	B (KG)	ϕ degrees
1	D.S.	100	-	-	-
2	Q_1-DH.	120	-476.13	-	-
3	D.S.	170	-	-	-
4	Q_2-FH.	190	287.95	-	-
5	D.S.	210	-	-	-
6	$(B.M.)_1$	264	-	8.843	28.45
7	D.S.	384	-	-	-
8	Q_3-FH.	424	197.24	-	-
9	D.S.	544	-	-	-
10	$(B.M.)_2$	598	-	8.843	28.45
11	D.S.	618	-	-	-
12	Q_4-FH.	638	469.19	-	-
13	D.S.	668	-	-	-
14	Q_5-DH.	688	-831.14	-	-

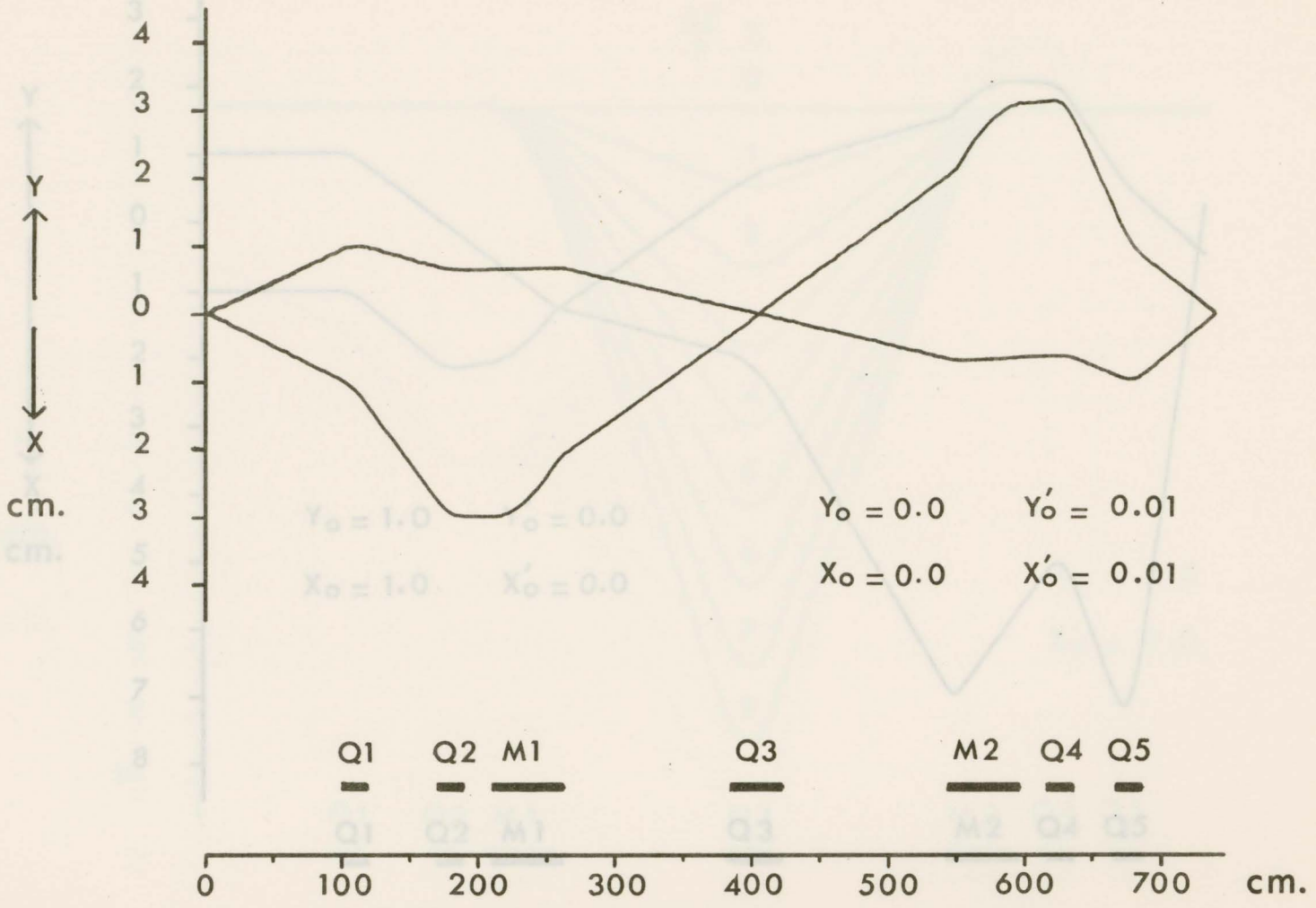

Fig. 22 Pion Channel, Sine-like Trajectories in the Horizontal and Vertical Planes

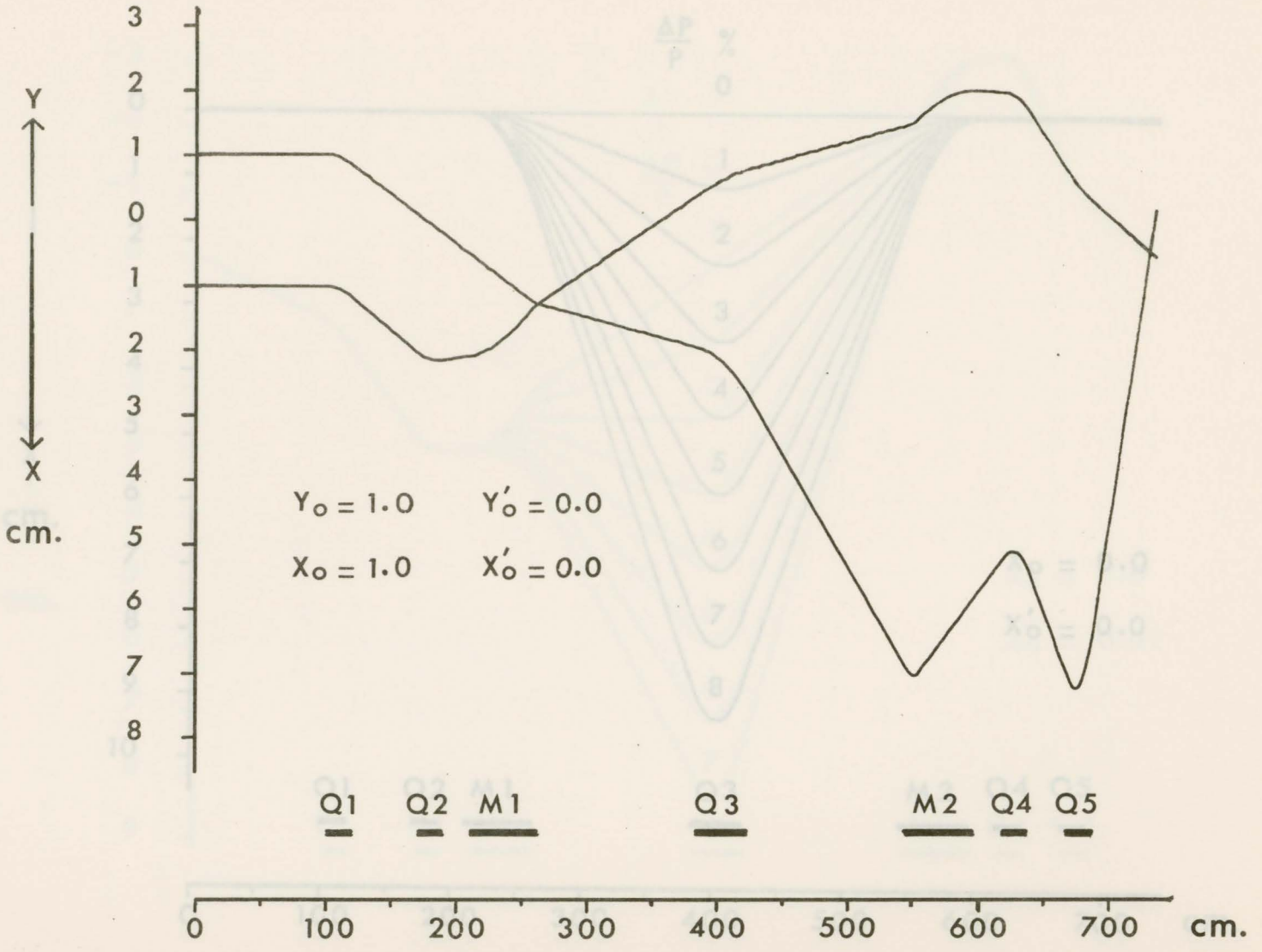

Fig. 23 Pion Channel, Cosine-like Trajectories in the Horizontal and Vertical Planes

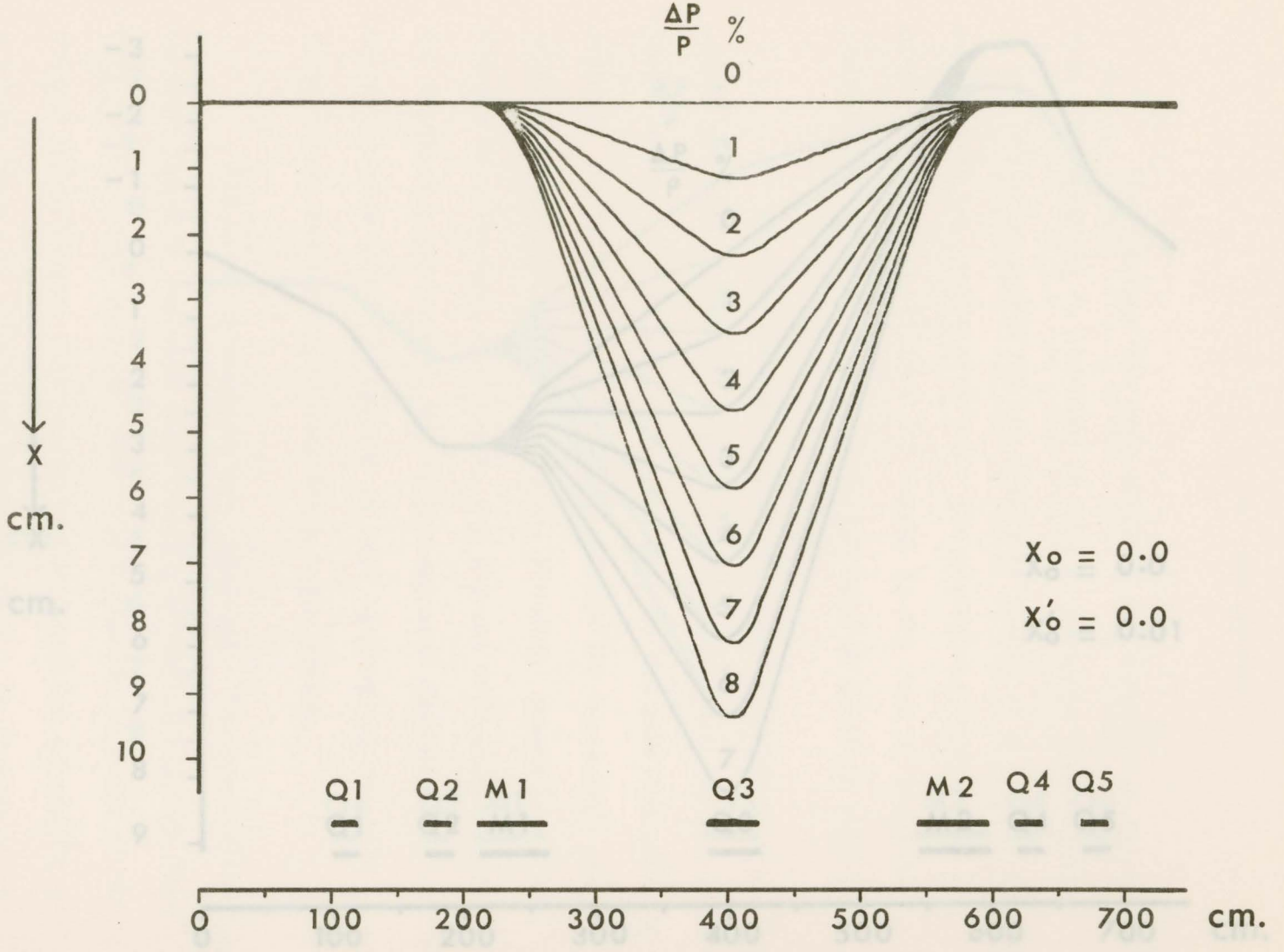

Fig. 24 Pion Channel, Dispersion Trajectories

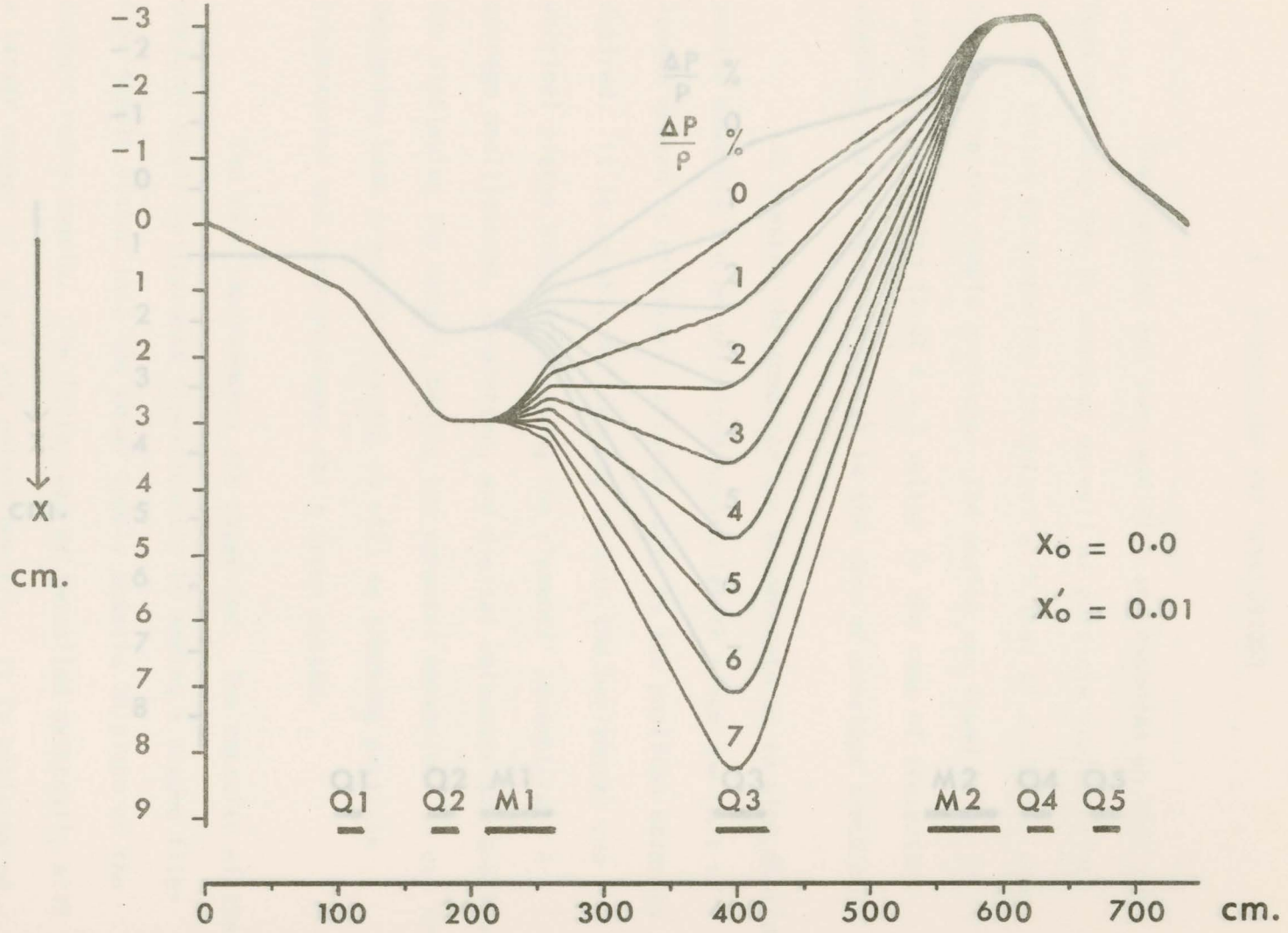

Fig. 25 Pion Channel, Sine-like Trajectories with Dispersion

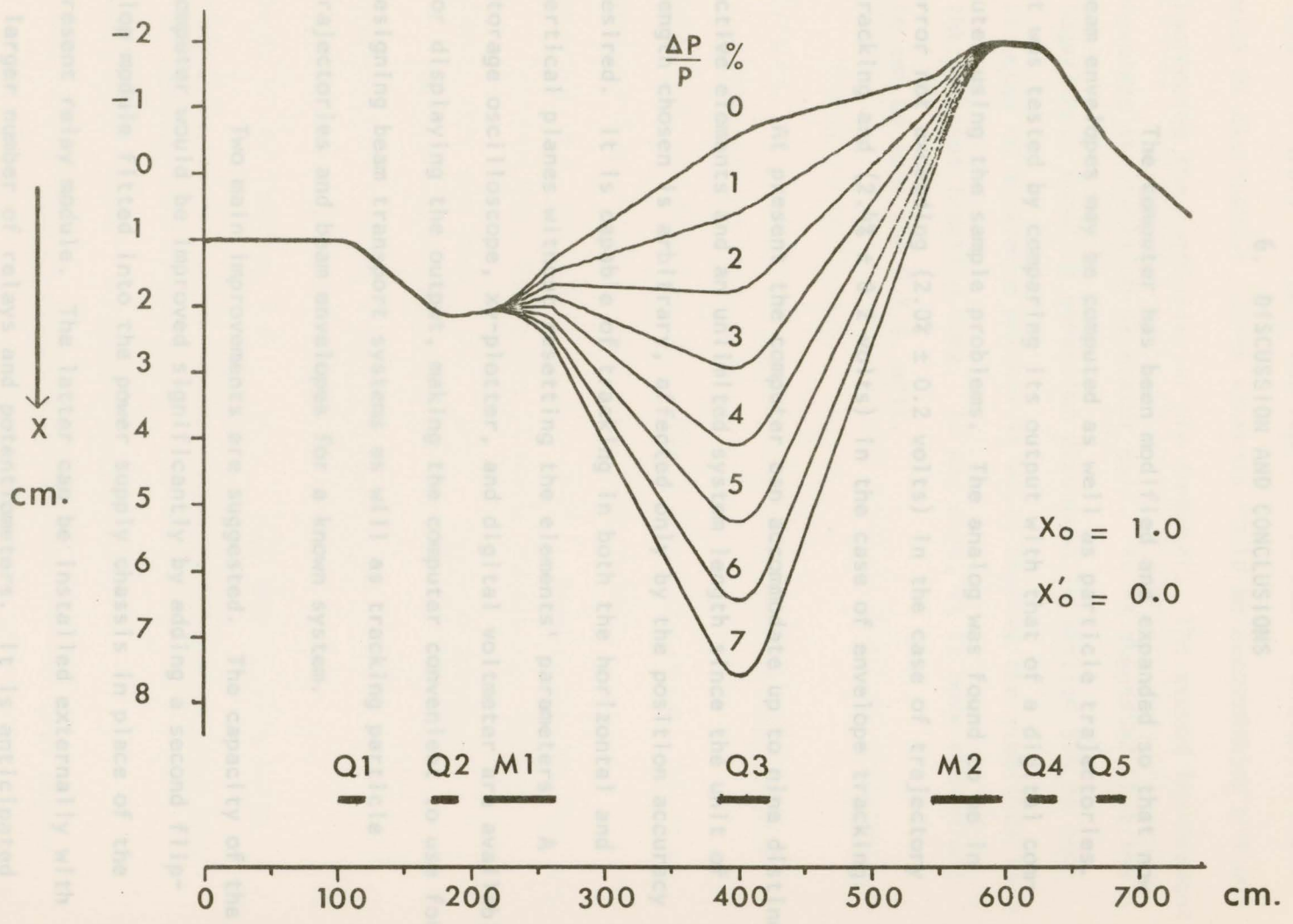

Fig. 26 Pion Channel, Cosine-like Trajectories with Dispersion

6. DISCUSSION AND CONCLUSIONS

The computer has been modified and expanded so that now beam envelopes may be computed as well as particle trajectories. It was tested by comparing its output with that of a digital computer using the sample problems. The analog was found to be in error not exceeding (2.0% ± 0.2 volts) in the case of trajectory tracking and (2.4% ± 0.2 volts) in the case of envelope tracking.

At present the computer can accommodate up to nine distinct active elements and an unlimited system length since the unit of length chosen is arbitrary, affected only by the position accuracy desired. It is capable of tracking in both the horizontal and vertical planes without resetting the elements' parameters. A storage oscilloscope, xy-plotter, and digital voltmeter are available for displaying the output, making the computer convenient to use for designing beam transport systems as will as tracking particle trajectories and beam envelopes for a known system.

Two main improvements are suggested. The capacity of the computer would be improved significantly by adding a second flip-flop module fitted into the power supply chassis in place of the present relay module. The latter can be installed externally with a larger number of relays and potentiometers. It is anticipated

that this would increase the capacity so that a transport system with 21 distinctive active elements could be accommodated without increasing the complexity of the computer. The second improvement involves the function generator unit. It is suggested that the logarithmic function generator discussed in Section 3.6 be constructed to determine whether it would improve the stability in the envelope tracking mode. In any case, it is more convenient to set up than the D.F.G. unit.

REFERENCES

Banford, A.P. 1966. The Transport of Charged Particle Beams. (E. and F.N. Spon Ltd., London)

Batho, H.F., Lobb, D.E., Robertson, L.P. and Warren, J.B. 1968. Proposal for an Engineering and Cost Study for a Radiobiology and Radiotherapy Facility Using a Negative Pi-Meson Beam from TRIUMF.

Brown, K.L. 1967. SLAC Report, SLAC-75, Stanford University, Stanford, California.

Gilbert, G.P. 1964. The Design and Use of Analog Computers. (Chapman and Hall, London)

Good, R.H. and Piccioni, O. 1960. Rev. Sci. Instr., 31, 1035.

Hansford R.N. 1965. AERE Report No. R 4869.

Hansford, R.N. and Aspley, R.J. 1967. Reprint No. 33, The Second International Conference on Magnet Technology, Oxford.

Huskey, H.D. and Korn, G.A. 1962. Computer Handbook. (McGraw - Hill, New York)

Jackson, A.S. 1960. Analog Computation. (McGraw - Hill, New York)

Kern, W. and Steffen, K.G. 1961. DESY Report, Desy-Noitz A 2.80

Korn, G.A. and Korn, T.M. 1956. Electronic Analog Computers. (McGraw - Hill, New York)

Lobb, D.E. 1968. Private Communication.

Louis, R.J. 1967. A Hybrid Analog Computer for Beam Optics Calculations. M.Sc. Thesis, University of Victoria, Victoria, B.C.

Montague, B.W. 1960. CERN Report, CERN 60 - 24.

Penner, S. 1961. Rev. Sci. Instr., 32, 150.

Rumphorst, F.R., Sonnemans, M.A.A., Arnold, H. and Koerts, L.A.Ch. 1967. Nuc. Instr. Meth., 50, 153.

Steffen, K.G. 1964. High Energy Beam Optics. (Interscience, New York)

Tautz, M.F. 1968 TRIUMF Report, TRI-68-8, University of Victoria, Victoria, B.C.

Vogt, E.W. and Burgerjon, J.J., editors. 1966. TRIUMF Proposal and Cost Estimate.

APPENDIX A. A DERIVATION OF THE ENVELOPE EQUATION

This derivation is developed briefly in Steffen (1964). The parametric form of the equation of the phase space ellipse is given as

$$\gamma u^2 + 2\alpha uu' + \beta u'^2 = \varepsilon \tag{A.1}$$

where $u = x$ or y and $u' = \frac{du}{dz}$.

If the envelope function E and its derivative with respect to z, E', are defined in terms of the ellipse parameters α, β, and ε as follows

$$E = (\varepsilon\beta)^{\frac{1}{2}} , \tag{A.2}$$

and

$$E' = \frac{dE}{dz} = \alpha(\varepsilon/\beta)^{\frac{1}{2}}$$

then from (A.2) we get $\beta = \frac{E^2}{\varepsilon}$ and $\alpha = -\frac{EE'}{\varepsilon}$

with

$$\gamma = \frac{1 + \alpha^2}{\beta} = \frac{\varepsilon^2 + E^2E'^2}{\varepsilon E^2} . \tag{A.3}$$

The negative sign was chosen in the expression for α since it always has the opposite sign to E', as seen in Figs. 4 and 5. Using (A.3) and (A.1), the ellipse equation becomes

$$\frac{\varepsilon^2}{E^2} u^2 + E'^2u^2 - 2EE'uu' + E^2u'^2 = \varepsilon^2 .$$

Differentiating with respect to z and dividing through by $(2E'u - 2Eu')$ gives

$$E''u - Eu'' - \frac{\varepsilon^2}{E^3} u = 0 \ . \qquad (A.4)$$

From the trajectory equation (2.3.1), with d = 0

$$u'' = - k(z)u \ . \qquad (A.5)$$

Substituting (A.5) into (A.4) and dividing through by u gives the envelope equation

$$E'' + k(z)E - \frac{\varepsilon^2}{E^3} = 0 \ .$$

APPENDIX B. ANALOG DETAILS

Before this work was started, the analog computer circuit was as shown in Fig. B.1. Since two amplifiers were required for the function generator unit, amplifiers 2 and 7 were removed from the computer, resulting in the analog circuit of Fig. 8. Their function as inverters is performed by relays as shown in Fig. B.2, where "FF" indicates a flip-flop and "RD" a relay driver.

In this modified circuit, the relay R5 has been added and other relays rearranged. The relay R4 controls the inputs to amplifier 3 instead of the output and will accommodate the types of elements given in Section 2.3.

In Fig. B.2 the connections are shown for three different elements, a quadrupole focussing in the x-plane "Q-FH", a quadrupole defocussing in the x-plane "Q-DH", and non-uniform bending magnet with $o<n<1$ and with normal entry and exit. Since a pole face rotation can be considered as a thin lens, it is connected as a separate element the same way as a quadrupole.

A quadrupole focussing in the x-plane is connected so that the signal from a relay driver energizing an RP1 type line simultaneously energizes the relay R2. All quadrupoles focussing in the x-plane are connected through diodes to the terminal R5-1

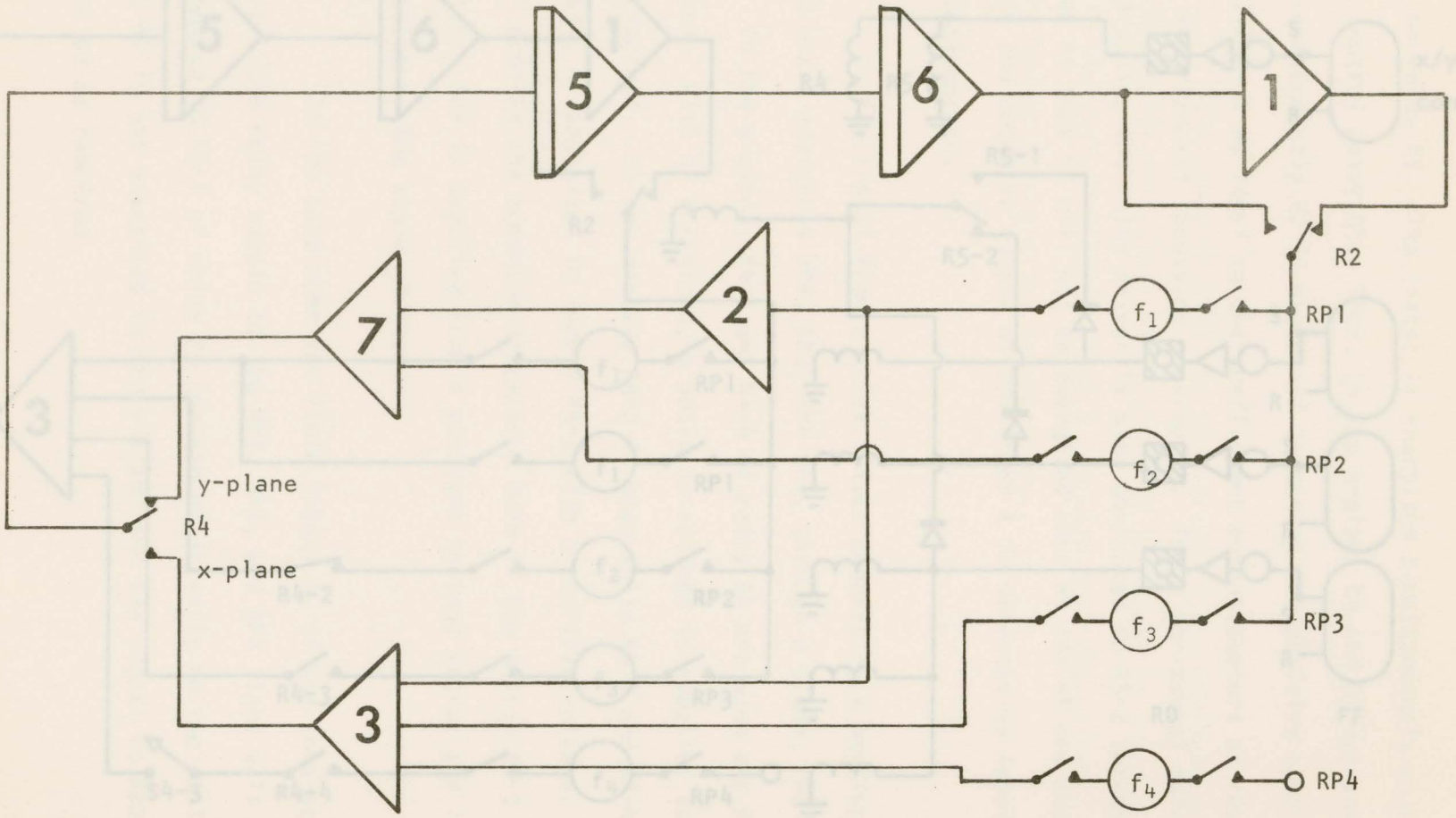

Fig. B.1 Analog Computer Circuit Before Modification

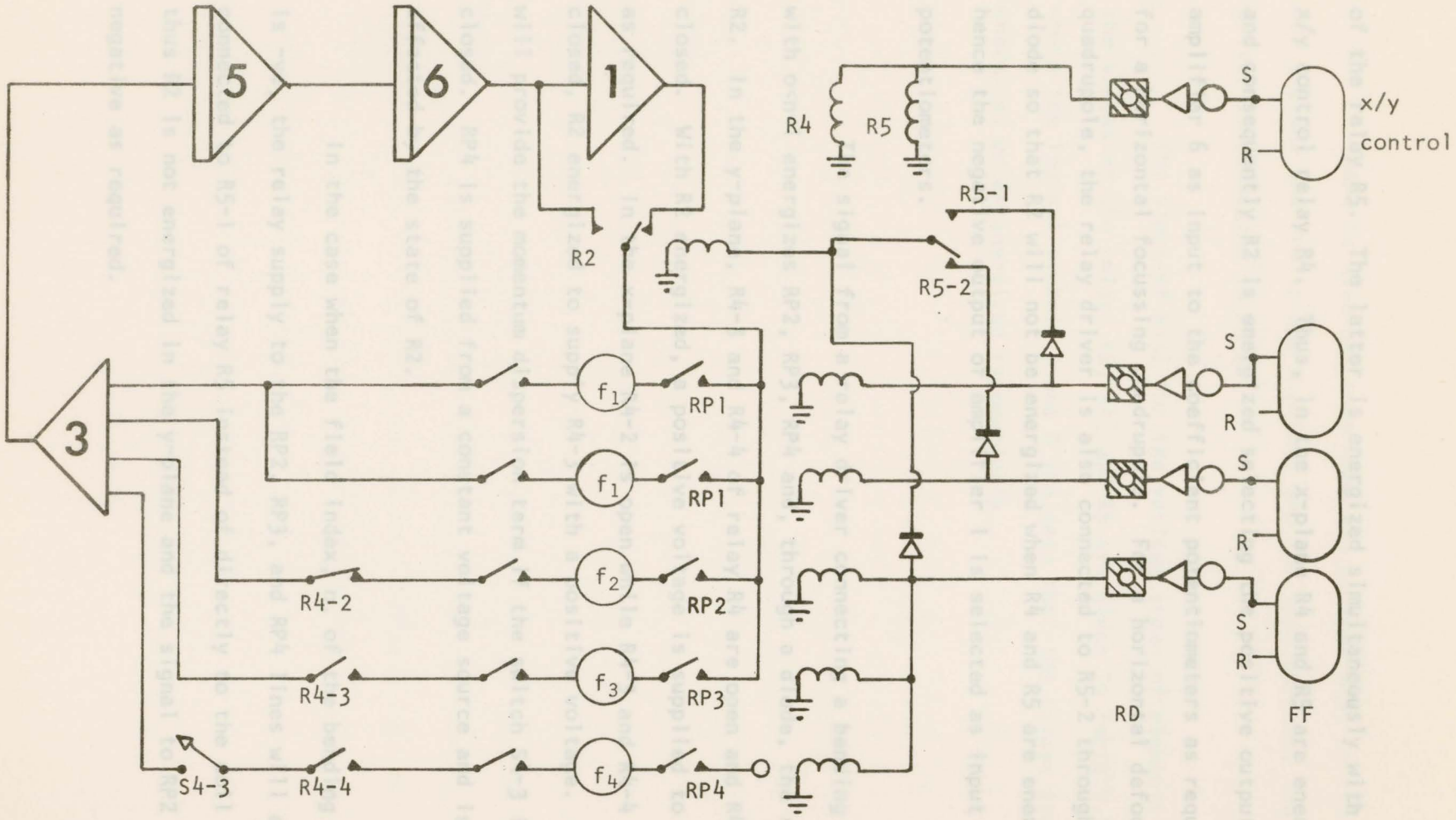

Fig. B.2 Modified Analog Circuit Showing Switching Arrangements for Various Types of Elements. All Relays are in the De-energized State.

of the relay R5. The latter is energized simultaneously with the x/y control relay R4. Thus, in the x-plane R4 and R5 are energized and consequently R2 is energized selecting the positive output of amplifier 6 as input to the coefficient potentiometers as required for a horizontal focussing quadrupole. For a horizontal defocussing quadrupole, the relay driver is also connected to R5-2 through a diode so that R2 will not be energized when R4 and R5 are energized, hence the negative output of amplifier 1 is selected as input to the potentiometers.

The signal from a relay driver connecting a bending magnet with $o<n<1$ energizes RP2, RP3, RP4 and, through a diode, the relay R2. In the y-plane, R4-3 and R4-4 of relay R4 are open and R4-2 closed. With R2 energized, a positive voltage is supplied to RP2 as required. In the x-plane R4-2 is open while R4-3 and R4-4 are closed, R2 energized to supply R4-3 with a positive voltage. RP4 will provide the momentum dispersion term if the switch S4-3 is closed. RP4 is supplied from a constant voltage source and is not affected by the state of R2.

In the case when the field index, n, of the bending magnet is -ve, the relay supply to the RP2, RP3, and RP4 lines will also be connected to R5-1 of relay R5 instead of directly to the coil of R2; thus R2 is not energized in the y-plane and the signal to RP2 is negative as required.

There is also the case when $n>1$ so that $k(z)$ is +ve in the y-plane and -ve in the x-plane, and for this purpose, the relay driver is connected to R5-2.

The signs of $k(z)$ for the various types of elements and the states of the relays R2, R4, and R5 are given in Table B.1, where the logical symbols 1 and 0 indicate that the relays are energized or de-energized respectively.

T A B L E B.1

Relay Logic for Various Types of Elements

Element Type	x-plane k(z)	x-plane d	x-plane R4	x-plane R5	x-plane R2	y-plane k(z)	y-plane R4	y-plane R5	y-plane R2
Q-FH.	$+\frac{g}{(B\rho)}$		1	1	1	$-\frac{g}{(B\rho)}$	0	0	0
Q-DH.	$-\frac{g}{(B\rho)}$		1	1	0	$+\frac{g}{(B\rho)}$	0	0	1
B.M. (1>n>0)	$\frac{1-n}{r_o^2}$	$\frac{1}{r_o}\frac{\Delta P}{P}$	1	1	1	$\frac{n}{r_o^2}$	0	0	1
B.M. (n=0)	$\frac{1}{r_o^2}$	$\frac{1}{r_o}\frac{\Delta P}{P}$	1	1	1	0	0	0	0
B.M. (n<0)	$\frac{1-n}{r_o^2}$	$\frac{1}{r_o}\frac{\Delta P}{P}$	1	1	1	$\frac{-n}{r_o^2}$	0	0	0
B.M. (n>1)	$\frac{1-n}{r_o^2}$	$\frac{1}{r_o}\frac{\Delta P}{P}$	1	1	0	$\frac{n}{r_o^2}$	0	0	1
Focussing Edge	$\frac{\tan\phi}{Lr_o}$		1	1	1	$-\frac{\tan\phi}{Lr_o}$	0	0	0

APPENDIX C. FUNCTION GENERATOR DETAILS

The diode function generator supplied by the Systron Donner Corporation consisted of two units with twelve segments each, six of which are for generating positive, and the other six, negative straight line segments. The segments were arranged in pairs as shown in Fig. C.1.

Because of the shortage of amplifiers available, and since only positive straight line segments needed to be generated, amplifier 1 was not required and the circuit was modified so that each unit contained twelve identical segments. Further, to increase the initial slope, some of the 634K resistors were replaced as discussed below, and finally, to increase the resolution of the break-point (bias supply) potentiometers, the 100 volts supply V_b was reduced to 9 volts for the first unit and 18 volts for the second. A typical segment of the modified D.F.G. is shown in Fig. C.2. The point B is left open-circuited in the first unit (segments 1 through 12) in order to increase the initial slope; it is grounded in segments 13 through 24, i.e. in the second unit. The resistor R has the values 250K for segments 1 through 6, 634K for segments 7 through 18, and 1 Meg for segments 19 through 24.

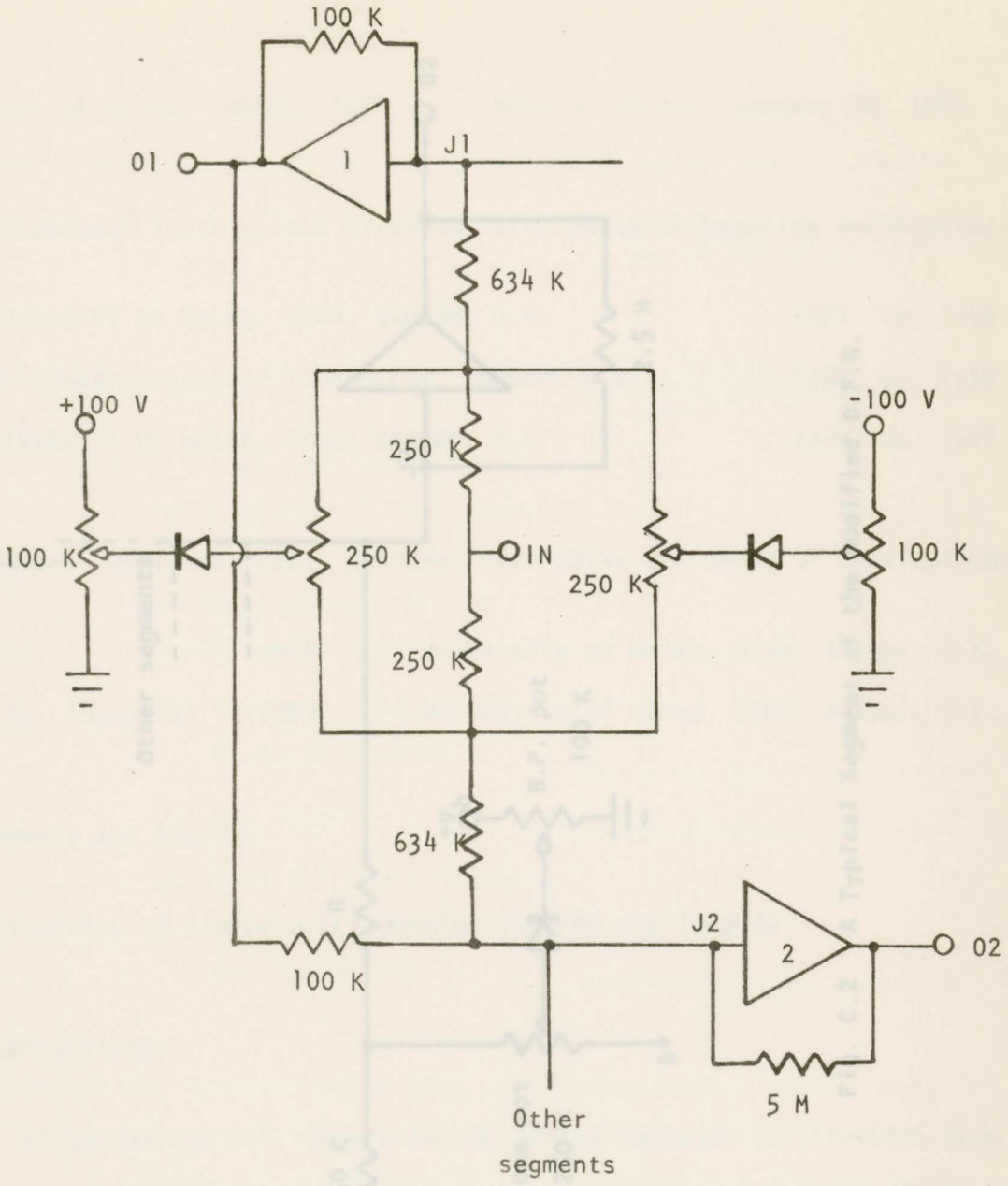

Fig. C.1 A Typical Pair of D.F.G. Segments as Supplied in Systron Donner Module 3351

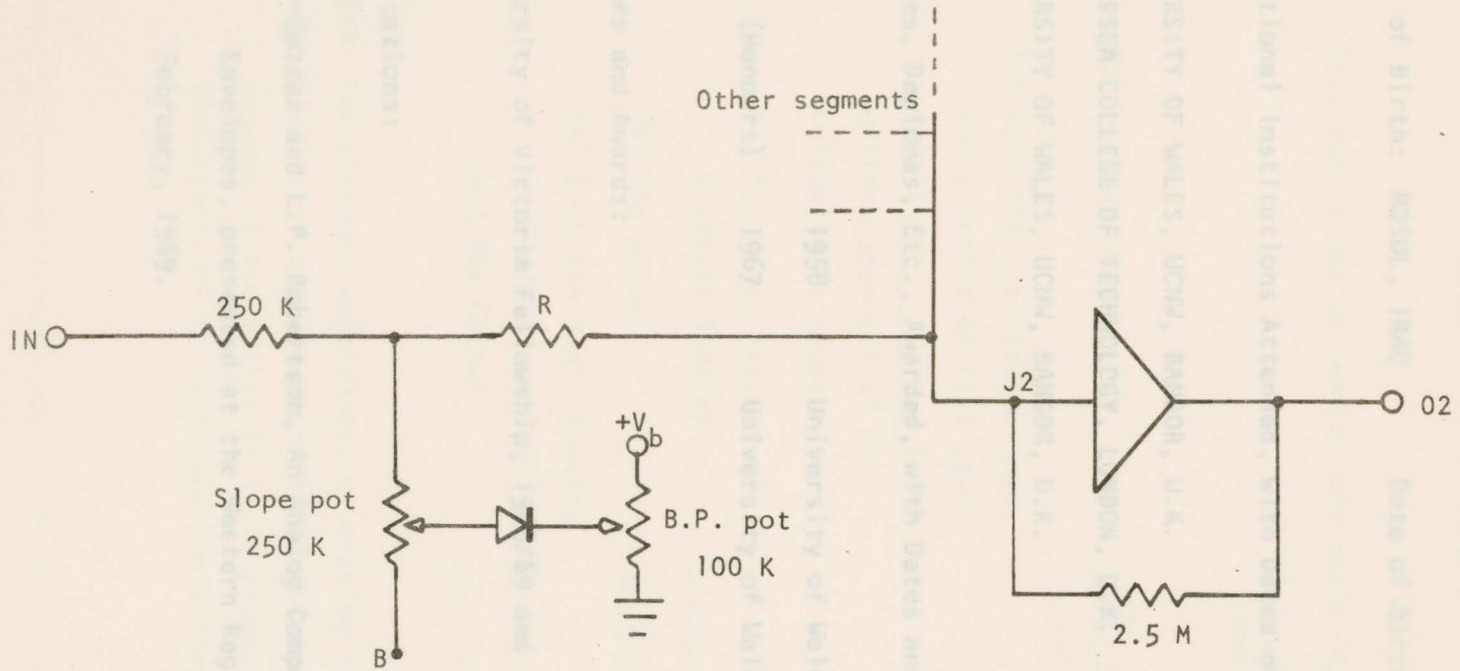

Fig. C.2 A Typical Segment of the Modified D.F.G.

Surname: AL-QAZZAZ Given Name: NADHIM

Place of Birth: MOSUL, IRAQ Date of Birth: January 30, 1935

Educational Institutions Attended, with Dates of Entering and Leaving:

UNIVERSITY OF WALES, UCNW, BANGOR, U.K.	1955 to 1958
BATTERSEA COLLEGE OF TECHNOLOGY, LONDON, U.K.	1958 to 1959
UNIVERSITY OF WALES, UCNW, BANGOR, U.K.	1965 to 1967

Degrees, Deplomas, Etc., Awarded, with Dates and Names of Institutions:

B.Sc.	1958	University of Wales, UCNW, Bangor, U.K.
B.Sc. (Honours)	1967	University of Wales, UCNW, Bangor, U.K.

Honours and Awards:

University of Victoria Fellowship, 1968/69 and 1969/70

Publications:

N. Al-Qazzaz and L.P. Robertson, An Analog Computer for Tracking Beam Envelopes, presented at the Western Regional Nuclear Conference, February, 1969.

Signature of Borrower	Address	Date

THE UNIVERSITY OF VICTORIA LIBRARY

MANUSCRIPT THESIS

AUTHORITY TO DISTRIBUTE

AUTHOR: This thesis may be lent or microfilm copies made available:

(signature of the author in one of the spaces below)

(a) Without restriction [redacted]

(b) With the restriction that, for a period of five years (until _____) the written approval of the following is required:

(1) The Dean, Faculty of Graduate Studies _____

(2) The Author _____

(3) Both the Dean, Faculty of Graduate Studies, and the Author _____

BORROWERS: The borrower undertakes, by signing below, to give proper credit for any use made of the thesis, and to obtain the consent of the author if it is proposed to make extensive quotations, or to reproduce the dissertation in whole or in part.

Signature of Borrower	Address	Date